THE USE OF THE WAVE GUIDE FOR DIELECTRIC MEASUREMENTS.

by

H. R. L. Lamont, M.A.,B.Sc.

Thesis

Submitted for the Degree of Ph.D.
to the University of Glasgow,
November, 1940.

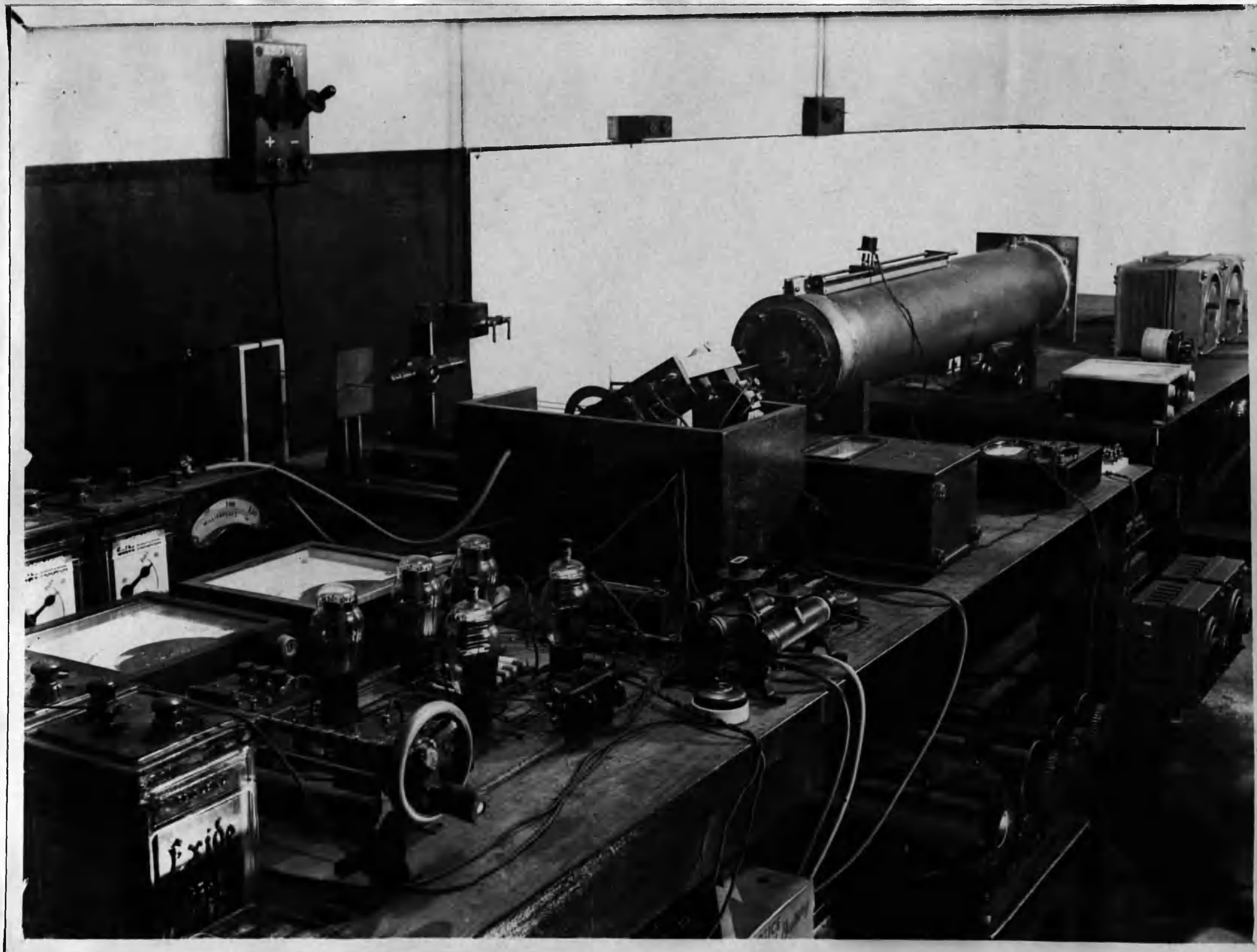

Fig. 1. View of complete apparatus.

PREFACE.

The work described in this Thesis was carried out during the sessions 1937-38 and 1938-39 in the Laboratories of the Natural Philosophy Department of the University of Glasgow. Although my subsequent appointment to a post in the Research Laboratories of the General Electric Co.,Ltd. prevented a continuation of this work during a third session, the Senate have kindly agreed to accept my candidature for the Degree of Ph.D., and for that decision I here express my gratitude.

The choice of subject was due to a suggestion from Dr. R. W. Sloane, of the G.E.C. Research Laboratories, who drew my attention to the papers which had recently been published on the subject of wave guides, and suggested that such wave guides would provide a useful means of investigating the dielectric properties of materials at very high frequencies. The suggestion was adopted, and I commenced the study of the problem, without, indeed, a definite scheme of work, but rather with the general aim of finding out how the wave guide could be used in dielectric measurements, what kind of results could be obtained by its use, and what, if any, were its advantages over other methods. Detailed answers to these questions are given in the text, but it may be said here that the idea proved a fruitful one, and a number of methods have been devised and useful results obtained.

Chapter I describes the preliminary investigations on the general propertied of wave guides and the apparatus used. A measurement of the dielectric constant of liquid paraffin is described in Chapter II. The method, a sound but clumsy one, is of basic importance. Chapter III is an interpolation in the general scheme. It is due to a suggestion by Dr. Thomson, that the dielectric constant of an ionised medium should be measurable by the method of Chapter II, and, although this investigation was abandoned after some difficulties had been experienced, that was rather because it seemed less important than the other projected work. Chapters IV and Vdescribe the most important methods which were developed of measuring the dielectric constant of both solids and liquids at frequencies of the order of 1500 Mc./sec. and above. In the final Chapter methods and results are compared and analysed.

The main lines of the Thesis have been published in two papers in the Philosophical Magazine*. It is from these that the printed figures used here have been taken.

The theory developed is original, and it has always been stated to what extent it depends on the work of others. The methods were devised by myself, although, as is stated in the text, they are to some extent adaptations of old methods to a new technique. On the other hand, investigations on dielectrics at these frequencies were very few, and the wave guide technique had not hitherto been used. Attention may be drawn to the methods described in sections 18 and 19. These are new and important methods, dependent upon an interesting mathematical result which I obtained in the theoretical study described in Chapter III. The preliminary theoretical treatment of the parallel wire line (section 14) seemed also to clear up some anomalies which became apparent in the works of some experimenters on dielectric constants. The apparatus was designed and assembled, and the experiments performed, by myself.

In conclusion, thanks are due to Dr. R. W. Sloane for the original idea for the work, to Prof. E. Taylor Jones for helpful guidance and liberal facilities, and to Dr. J. Thomson for constant valuable advice and discussion.

Wembley,
November, 1940.

* "Theory of Resonance in Microwave Transmission Lines with Discontinuous Dielectric", Phil. Mag. 29 521 (June 1940)
"The Use of the Wave Guide for Measurement of Microwave Dielectric Constants", Phil. Mag. 30 1 (July 1940)

CONTENTS

Chapter 1.

BASIC IDEAS AND EXPERIMENTS.

During the latter part of the year 1936 there were published in America three papers dealing with the transmission of electromagnetic waves through hollow metal tubes. These were the first thorough theoretical and experimental studies of a problem which, nearly forty years before, had been studied in an idealised form by Lord Rayleigh. The reason for the lapse of time between the two was the lack of oscillators suitable for generating the high frequencies which were essential for the use of such tubes.

The standard conducting systems of electromagnetic energy, the parallel wire and concentric tube systems, have long been used for the measurement of dielectric properties of materials, and it seemed that this new transmission system might provide means of overcoming some of the difficulties experienced with the others at high frequencies, and an attempt at the application of its properties to such measurements would prove a useful line of research. Accordingly work was commenced on the general programme of the investigation of how wave guides - the transmission system has come to be called by this name - could be utilised in the problem of measuring values of dielectric constant at high frequencies.

As the generation and detection of waves in tubes was a new technique whose possibilities had been by no means fully explored in the published papers, and as the technique of the generation of suitably short waves was also recent, much preliminary work had to be done. An outline of this work is given in the succeeding sections of Chapter 1.

1. Components of the Apparatus.

The oscillator chosen was a magnetron, type Osram CW10, which was capable of producing electronic oscillations up to frequencies of 2000 Mc./sec., corresponding to a wavelength of 15 cm. The filament and magnetic field currents for the oscillator were provided by accumulators, and the anode potential was supplied through a potentiometer system from a high tension motor generator. Parallel wires fixed to the anode leads and fitted with a movable shorting bridge form the anode circuit of the valve, which is tuned to resonance with the electronic oscillations generated in the valve. The circuit of the oscillator is shown in fig. 2.

An important property of the wave guide is that it will not transmit waves of frequency less than certain critical values defined by the tube radius and the material filling it. Considering the upper frequency limit of the oscillator and the dielectric materials likely to be used it was decided that a tube with an internal diameter of about 7 inches would be most suitable. Accordingly a tube was procured made of 10 gauge copper, seven inches internal diameter and five feet long.

A simple wavemeter was made up, consisting of two

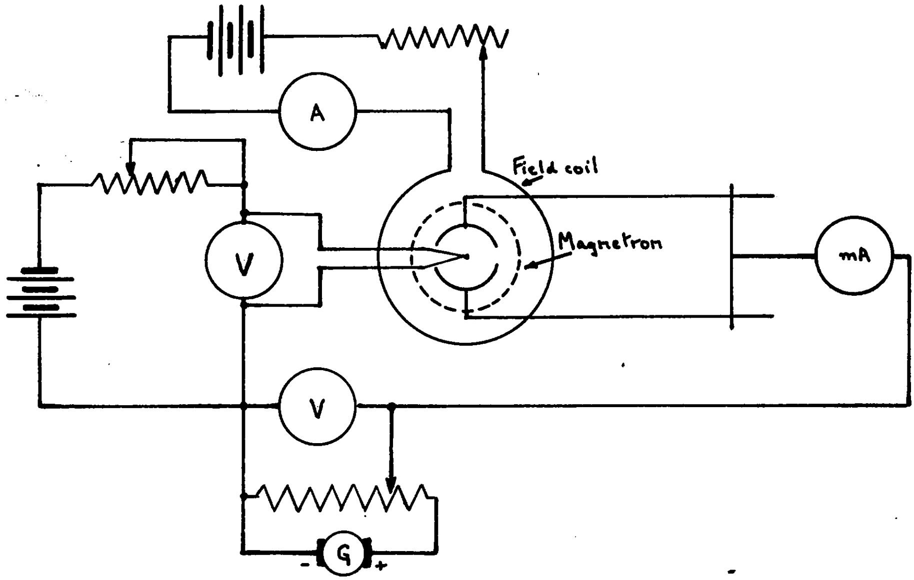

Fig. 2. Magnetron oscillator circuit.

parallel wires, bridged at one end, and carrying a movable bridge which included a small flash-lamp bulb as an indicator of resonance. When the wavemeter was coupled to the magnetron circuit the bulb glowed for positions of the bridge differing by one-half wavelength.[1,2,3]

Before proceeding further with the arrangement of the apparatus it will be helpful to give a short summary of some of the theory of propagation in wave guides.

2. Brief Theory of Wave Guides.

Electromagnetic waves may be propagated through a single hollow tube of any section, subject to certain conditions. A series of characteristic wave-forms is possible, there being a limiting frequency for each type below which no propagation occurs. For circular tubes in particular the free space wave-length corresponding to a limiting, or critical, frequency for a tube of radius a is given by $\lambda_c = \frac{2\pi\sqrt{\varepsilon}}{k}$, where ε is the dielectric constant of the material filling the tube and k has a value statisfying the equation

$$J_\nu(ka) = 0$$

or the equation

$$J_\nu'(ka) = 0 \qquad \left(\text{i.e. } \frac{d}{d(ka)} J_\nu(ka) = 0\right).$$

$J_\nu(ka)$ is the Bessel function of the first kind of integral order ν.

The largest values of λ for the respective equations are

$$\lambda = 2{\cdot}61\, a\sqrt{\varepsilon} \qquad (1)$$

and

$$\lambda' = 3{\cdot}41\, a\sqrt{\varepsilon}, \qquad (2)$$

thus limiting practical applications to micro-waves.

The wave-length inside the tube is not $\lambda/\sqrt{\varepsilon}$ as for a parallel wire system, but is given for the ideal non-dissipative case by the equation

$$\frac{1}{\lambda_t} = \sqrt{\frac{\varepsilon}{\lambda^2} - \left(\frac{k}{2\pi}\right)^2} . \qquad (3)$$

Also the wave inside the tube is not a plane wave; there exists always a component of electric intensity or of magnetic intensity or of both in the direction of propagation. Waves are broadly classifiable as types E and H. E-waves are those depending on solutions of $J_\nu(ka) = 0$ and have zero axial magnetic force; H-waves depend on solutions of $J_\nu'(ka) = 0$ and have zero axial electric force.

The wave forms of the first two principal waves of the E and H types are shown in fig. 3. To excite any particular wave an input arrangement must be used which will produce lines of force approximating to those of the desired wave type. For example, a rod projecting along the axis of the tube and excited externally will produce the E_0 type of wave.

3. Arrangement of Apparatus and Preliminary Experiments.

Fig. 4a is a schematic diagram of the layout of the apparatus as first used. A metal disk having an insulating bush at its centre was fixed to one end of the tube. This carried a rod acting as exciting device for the E_0 -wave. The ends of a short parallel wire transmission line coupled to the oscillator were connected to the rod and to the tube wall. As detector of the wave a 10 ma. thermojunction connected to a microammeter was used. It was found by trial

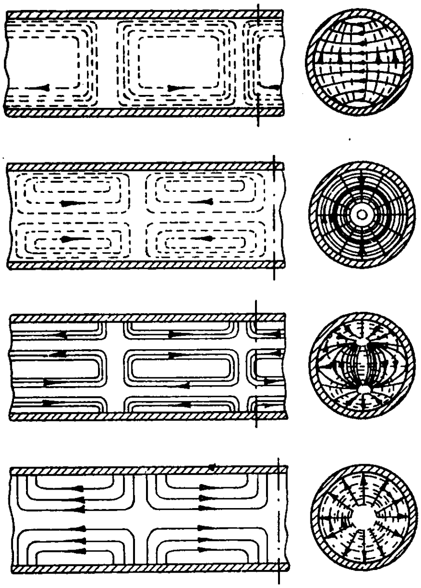

Fig. 3. Illustrating the four principal types of wave; in descending order they are E_0, E_1, H_0, H_1. (From Bell Syst. Tech. J. 15 288 (1936).)

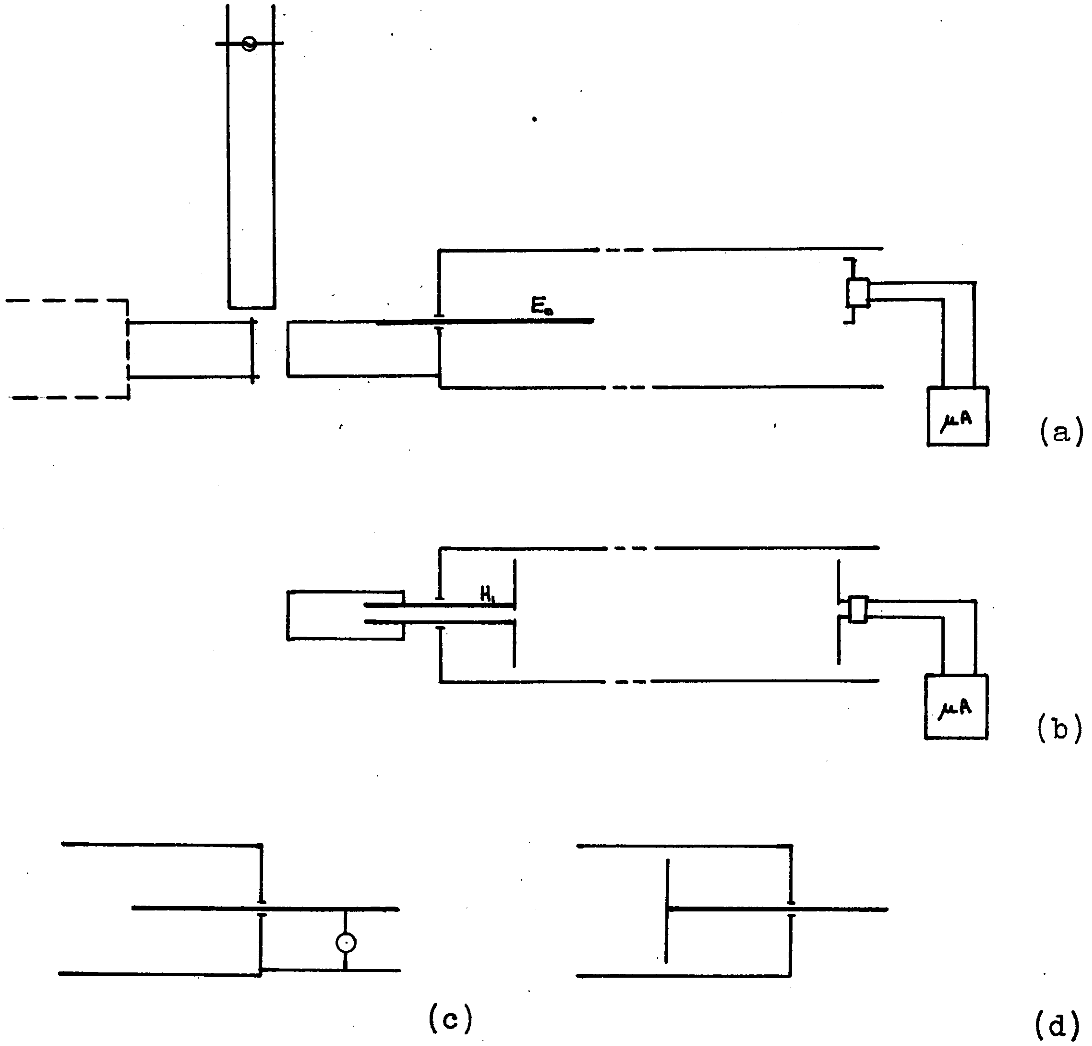

Fig. 4. Various launching and detecting arrangements.

that the most sensitive pick-up arrangement was as shown in fig. 4a - a pair of wires connected to the heater of the thermojunction and bent at the ends, one end being along the axis and the other near the tube wall. It was found that when the wavelength of the oscillator was varied about the cut-off point for the wave, the critical point could be accurately determined by the detector. This was found to occur at $\lambda = 23\cdot3$ cm. The theoretical value given by (1) is 23·2 cm., which agrees closely with the experimental value.

The H_1-wave was then generated and detected by means of the arrangements shown in fig. 4b. The cut-off wavelength was here found to be 30·1 cm., to which the corresponding theoretical value is 30·3 cm.

When the tube is filled with a liquid dielectric both ends must be closed, and so an attempt was made to detect an E_0-wave with the arrangement shown in fig. 4c, which is similar to the exciting device. A rod is arranged to move along its axis and the position of the thermocouple along the rod is altered till maximum sensitivity is attained. This was found to work quite successfully.

For the purpose of investigating the wave distribution a longitudinal slot was cut in the tube parallel to the axis, and a slider arranged to move on guides over the slot, its displacement being read on a scale. The slider carried a 5 ma. thermojunction from which a probe projected into the interior of the tube. From readings on a microammeter connected to the thermojunction the radial field distribution along the length of the tube can be plotted. This slot should not materially affect the field for E-waves, as for these types conduction currents in the tube walls are everywhere along the generators.

To set up a stationary wave system in the tube a metal reflecting plate was arranged as a moving piston at the end of the tube - fig. 4d. When the piston is moved to a position of resonance stationary waves are set up, and the wavelength in the tube can be found by measuring the distance between successive maximum indications on the slider thermojunction. In practice such measurements proved to be vitiated by the presence of other subsidiary maxima due to the principal and possibly other wave types.

4. Modifications to the Apparatus.

The above preliminary experiments indicated that the theoretical wave types could be produced, and that the apparatus could be used for quantitative measurements. Some modifications were obviously necessary, the chief being, (a) a means of stabilizing the oscillator output, which varied considerably with fluctuations of mains voltage, (b) a wave launching mechanism giving as nearly as possible a single pure type of wave, (c) a better means of providing variable coupling between this mechanism and the oscillator, and (d) a more accurate wavemeter. The means of realization of these requirements will now be described.

(a) As the magnetron output is very susceptible to changes in anode potential a means is required of compensating for random fluctuations of anode potential while at the same time allowing this potential to be set to any desired value in a range of about 500 to 2000 volts. Suitable circuits had been developed, and one described by Nergaard[4] was chosen. The circuit is shown in fig. 5, and consists of three paralleled triodes in series with the anode supply. The grid potential of the triodes is supplied through two steep-slope pentode amplifier stages connected across the output, and the feedback from these to the triodes is such that variations in the input voltage affect only the voltage drop across the triodes and leave the output unaffected. Variation of the output voltage is by adjustment of the variable resistances shown. The unit proved very satisfactory in operation, changes in output being about 1 per cent for a 100 per cent change in input. The output voltage is independent also of the current taken. This stabilizer, in conjunction with large and well-charged accumulators for filament and field currents, gives satisfactory stability over the short period required for any set of measurements.

(b) The chief disadvantages of the wave launching methods so far used is that they have to be adjusted to avoid spurious waves. Types have been described by Southworth[5] which will produce a substantially pure wave-form, and sections of them are shown in fig. 6. Metal end plates of this form were made and could be placed over the end of the tube and kept in place by a trolitul insulating plate. The high-frequency generating potential is applied across the points shown by dots.

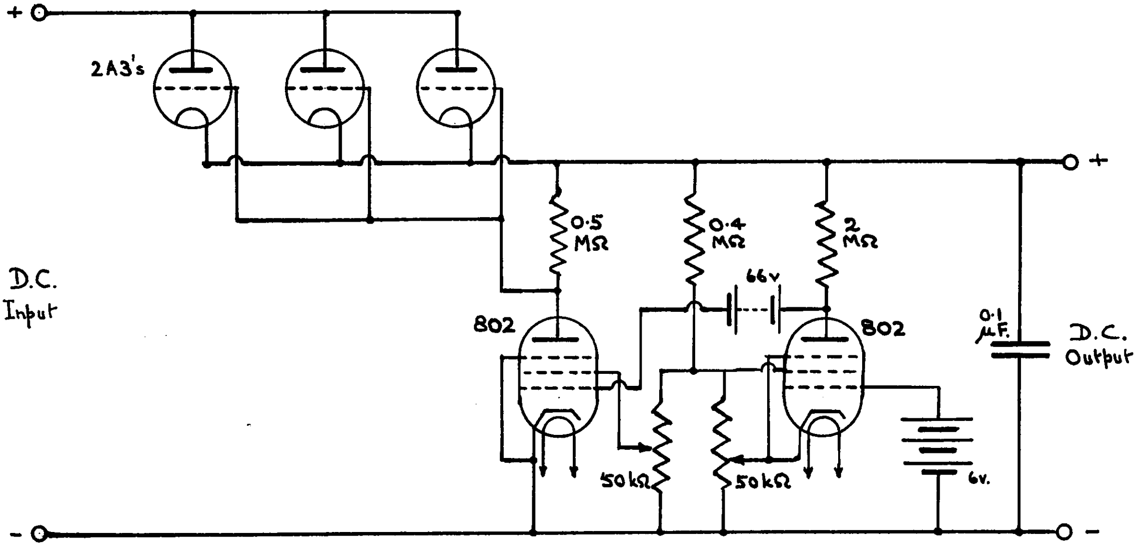

Fig. 5. Circuit of stabilizing unit.

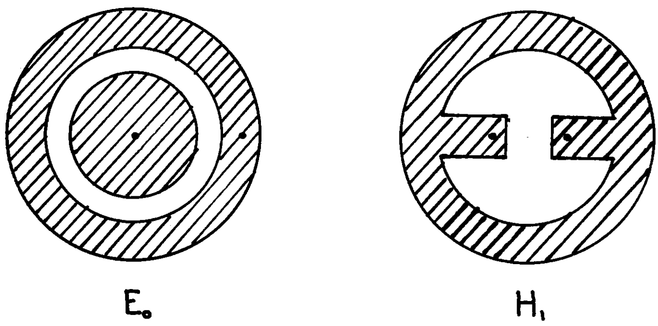

Fig. 6. Sections of launching devices for E_0 and H_1 waves.

(c) The anode circuit of the magnetron is a pair of parallel wires attached to the anode leads and fitted with a sliding bridge for tuning purposes. To facilitate the coupling of this circuit to the wavemeter and tube system the bridge was kept fixed and the magnetron made movable upon rails. Coupled loosely to the fixed end of the anode circuit and at right angles to it is the wavemeter. For the generation of E_0-waves coupling to the oscillator is by means of a trombone arrangement fixed between the ring and the disk of the arrangement of fig. 6. The trombone length can be varied to tune the coupling line to one-quarter wave-length, and the tube can be moved on rollers to vary the degree of coupling. Later it was found quite satisfactory to omit the side of the trombone which connects to the tube, the remaining L-shaped part giving adequate coupling. Actually the anode circuit and tube coupling line are not coplanar, their planes being parallel and about 1 cm. apart, to allow free movement of the anode circuit. At the other end of the tube is a movable piston sliding in a bush with liquid-tight gland fixed in a trolitul end-plate. The piston head is a disk of diameter slightly less than the internal diameter of the tube, and contact between the piston head and the walls of the tube is maintained by 24 phosphor-bronze springs arranged round the periphery of the piston head. By means of a scale, displacements of the piston can be measured.

(d) The improved wavemeter consists of two parallel copper wires, closed at the coupled end, carrying a brass reflecting plate through which the wires pass in close-fitting holes. The plate is moved by a screw and its position read by a travelling microscope. A vacuum thermo-junction connected to a microammeter is fixed near the coupled end. The distance between two successive positions of the reflecting plate which produce a maximum deflection on the microammeter represents a half wave-length. The length of the parallel wires allows three to four half wave-length measurements, and these are consistent to about 0·1 per cent. The corrections to be applied for wire spacing and skin effect have been discussed by Hund[6], and his equations are applied here.

If d is the wire diameter, a the spacing between the wires, and p the angular frequency, then the velocity of propagation of waves along parallel wires is reduced from the velocity of light in the ratio $(1-\Delta)/1$ by skin effect and proximity effect, where Δ is given by the equation

$$\Delta = \frac{\sqrt{r}}{8 \log_e \frac{1+\sqrt{1-(d/a)^2}}{d/a} \cdot \sqrt{p\{1-(d/a)^2\}}} \quad (4)$$

and r is the direct current resistance per cm. length in e.m. c.g.s. units. For the wavemeter $d = 0{\cdot}163$ cm., $a = 4{\cdot}2$ cm., and $p \sim 2\pi . 10^9$, and thus

$$\Delta \sim 1{\cdot}5 . 10^{-4}.$$

So the difference between the wavelength measured on the wavemeter and the actual free-space wavelength is of the order of 0·015 per cent, which is quite negligible.

A sectional drawing of the apparatus is given in fig. 7, and fig. 1 is a photograph of the complete layout. The mag-

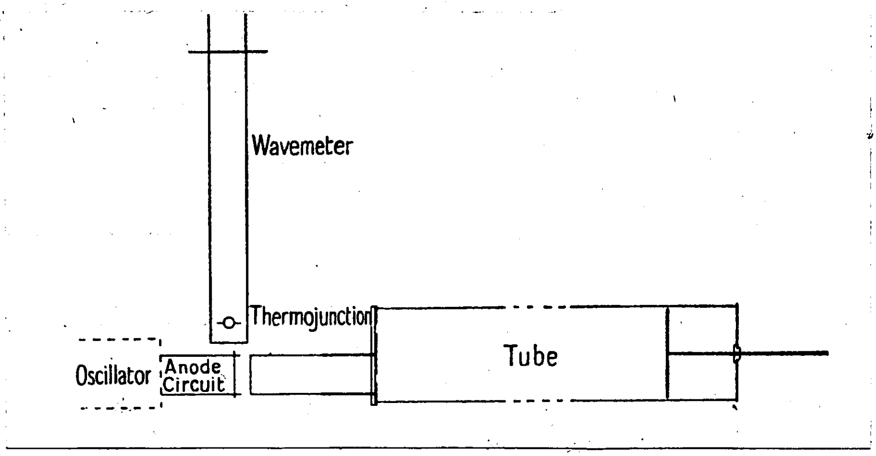

Fig. 7. Diagrammatic view of apparatus layout.

netron is contained in the box in the centre of the photograph, while in front of it are the field and filament accumulators, rheostats and meters, and the stabilizing unit. Under the bench are the controls for the motor generator which supplies the anode current, and the potentiometer voltage control. To the left of the box is the wavemeter, and behind it the tube with the E_0 -wave launching arrangement and the sliding thermojunction in position.

To test the apparatus a comparison was made between oscillator wavelengths as determined by the wavemeter and by tube measurements. The measurements made showed agreement with wavemeter readings to less than 0·25 per cent at a number of points in the range 15 to 22 cm.

Chapter 2.

MEASUREMENTS ON LIQUID DIELECTRIC.

5. Background of Previous Measurements.

Many measurements of dielectric constants at high frequencies have been made since the time of Drude, whose classic experiments are the basis of most of these. Drude[7] used the resonant properties of the Lecher wire system coupled to a high-frequency oscillator. In his "first method" the wave-length along the wires was measured, first in the air, then with the wires immersed in liquid of dielectric constant ε . If λ_1 and λ_ε are these respective lengths, ε is given by the relation $\lambda_1 = \sqrt{\varepsilon}\,\lambda_\varepsilon$. In Drude's "second method" a simple form of condenser filled with the liquid to be measured was placed across the ends of the parallel wires and the resultant resonant length found. The condenser was calibrated in terms of known liquids.

A source of inaccuracy in all such experiments is the impossibility of including the complete electromagnetic field surrounding the wires. This error is removed when the Lecher wires are replaced by a pair of concentric tubes. The field then exists entirely between the tubes, and the outer serves as a screen. Drake, Pierce, and Dow[8] have used such a system for measurements on water by Drude's first method, and Kalinin[9] has used Drude's second method with similar apparatus.

The wave guide has the same advantages as those noted above for the concentric line, and its properties make it very suitable for the investigation of high-frequency dielectric constants, but, with the exception of some elegant measurements by Kašpar[10] with dielectric guides, the little experimental work so far published has been directed to the production and detection of the waves and to verification of the theory.

6. Dielectric Measurements with Liquid Paraffin.

In order to test the wave guide method of measurement it was desirable to choose a liquid having small losses (since the simple theory assumes a loss free dielectric), and one about which suitable information was available. Liquid paraffin had been used at somewhat longer wavelength by other experimenters, and is a non-polar dielectric which should not show dispersion or large losses. Its physical properties also make it a convenient substance, and accordingly liquid paraffin was chosen for attempted measurements of its dielectric constant at wavelengths of the order of 20 cm.

The two methods used in the case of air suggested themselves; the first to determine the critical wavelength and find ε from equation (1), the second to measure λ_t and λ at values of λ less than its critical value, and use equation (3). The first method is the limiting case of the second.

The apparatus in its improved form was used, and the tube was filled with pure liquid paraffin. Small ridges soldered to the edges of the longitudinal slot allowed the tube to be filled completely without overflowing. The wave launching mechanism first used was that to produce E_0 -waves. Waves of this type were easily detected using the arrangement of fig. 4c, and the cut-off wavelength was found to be about 33•6 cm. Here the cut-off was not so sharp as when the tube contained air, which results in some uncertainty as to the value of the critical wavelength. If 33•6 cm. is taken as the critical wavelength, then the value of the dielectric constant of liquid paraffin given by (1) is 2•09. The lack of sharpness of the cut-off, which is due to modification of the simple theory by dielectric loss, makes this method of little use for accurate work. However it is only in this limiting case that small losses produce large effect, and it was expected that the second method could be used with success.

To use the second method the magnetron was set up at a wavelength well below the above critical value, and by means of the moving probe the axial distribution of electric field along the tube was plotted. At first complicated curves were obtained showing the co-existence of several types of wave, but by adjustment of the reflecting piston and loosening of the input coupling a simple waveform could be produced. Fig. 8 shows two typical curves, the first of which consists of several unresolved components, while the second is the pure waveform which can be finally attained. The oscillator wavelength for these two curves was 24•0 cm. The distance between

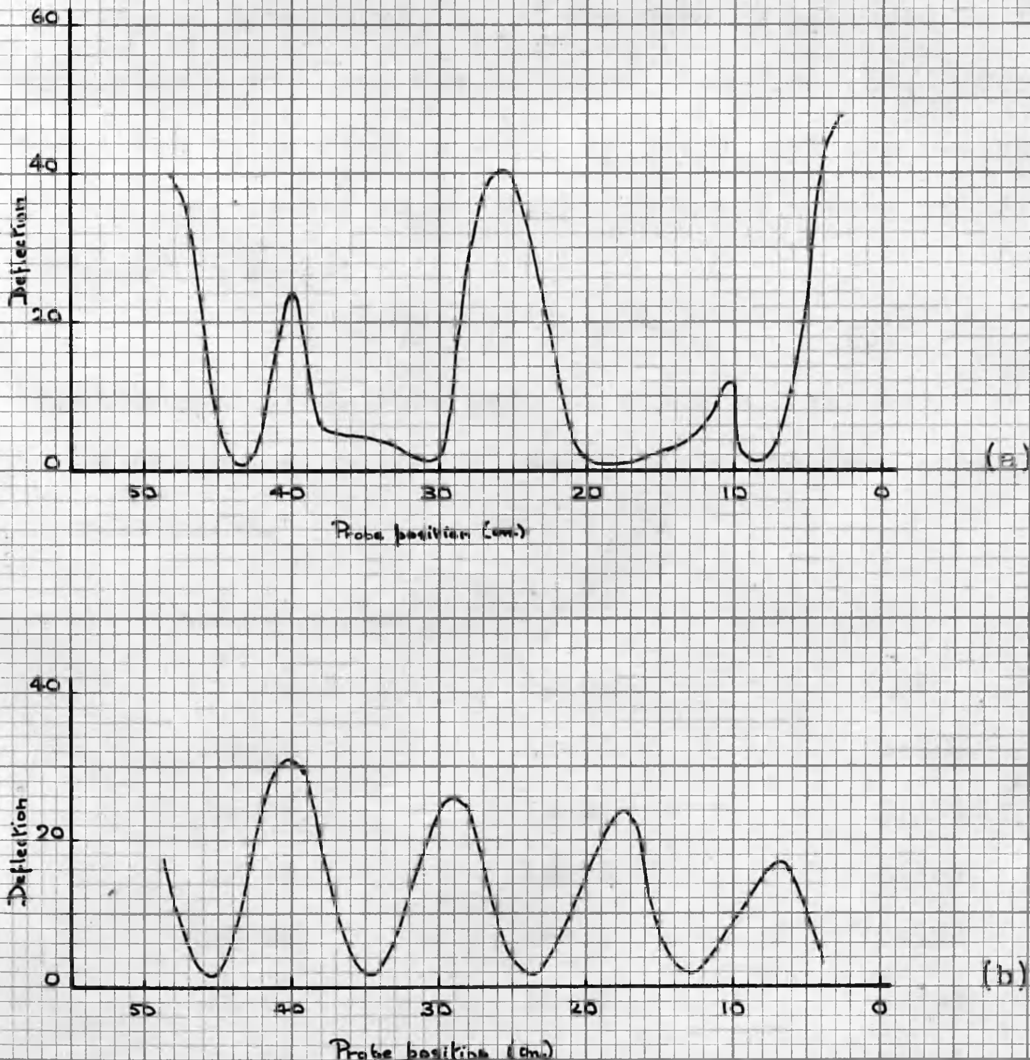

Fig. 8. Longitudinal wave distribution--H_0 wave.

two maxima or minima on a curve such as fig. 8 (b) gives half the wavelength in the tube, i.e. $\frac{1}{2}\lambda_t$. If the free-space wavelength, λ, of the wave is measured on the wavemeter, ε can now be calculated from (3). For E_0-waves the value of ka is given by 2·405, and the radius a of the tube is 8·9 cm. Inserting these values in (3) and rearranging we get

$$\varepsilon = \lambda^2\left(1/\lambda_t^2 + 0{\cdot}00184\right). \qquad (5)$$

Measurements of λ_t were made at different values of λ. These are given in the following table and from each pair ε is calculated.

Table 1.

λ (cm.)	λ_t (cm.)	ε
16·14	12·30	2·201
16·97	13·25	2·171
17·65	13·90	2·187
18·08	14·35	2·189
18·61	15·05	2·168
18·88	15·20	2·198
20·23	16·85	2·193
20·81	17·40	2·225
21·51	18·60	2·188
22·64	20·25	2·196
23·84	22·40	2·178
24·79	24·14	2·193
	Mean.	2·191 ± 0·003

It was discovered that at about $\lambda = 24$ cm. there was present in the tube a strong component of the first wave of the H_2 series. For this series $k = 3{\cdot}04/a$; 3·04 being the first zero of $J_2'(x) = 0$. Values of ε obtained for this wave are given in table 2.

Table 2.

λ (cm.)	λ_t (cm.)	ε
23·07	30·4	2.15
23·93	35·1	2·21
24·29	38·1	2·18
24·61	42·1	2·15

Corresponding values of λ, λ_t are plotted as co-ordinate points in fig. 9, the curves through the points being the curve of equation (3) for ε equal to the mean value obtained for each set of points.

For H_1 -waves the launching device shown in fig. 6 was used, and again values of ε of the order 2·2 were obtained. The results for H_1- and H_2- waves show a wider dispersion than those for E_0- waves. This is to be expected from the disturbing effect on the field of the slot in the tube. For E-waves the currents in the tube walls are parallel to the generators, while for H-waves there are in addition circulating currents round the tube. The effect of the slot will be to distort this latter current.

For reference the method used here will be called method A; the mean result obtained for the dielectric constant of liquid paraffin at wavelengths between 16 and 25 cm. is

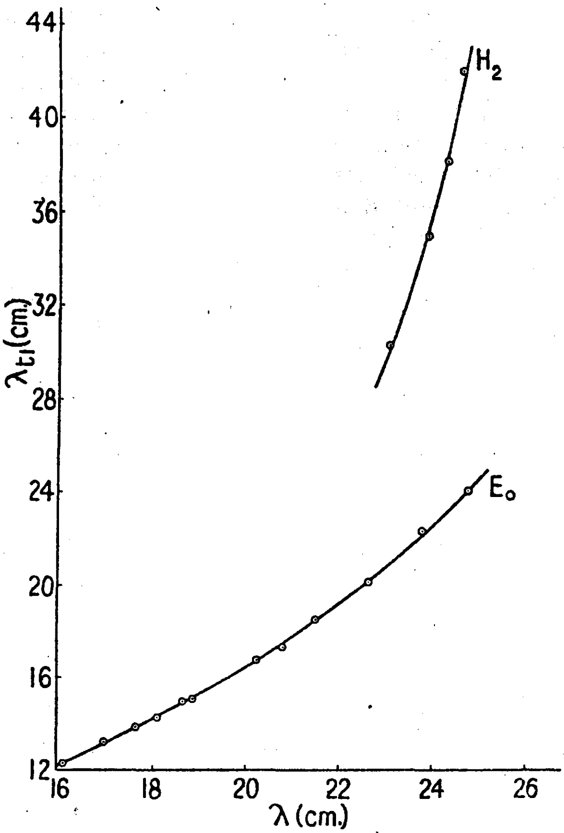

44
40
36
32
28
24
20
16
12
λ_{t1}(cm.)
16
18
20
22
24
26
λ (cm.)
H_2
E_0

Fig. 9.

$2{\cdot}191 \pm 0{\cdot}003$.

7. Comparison with Results by Standard Methods.

As a check on the above result a measurement was made by the classic method of measuring the wavelength of waves along two parallel wires immersed in the dielectric. For this purpose a large trough was used, some six feet long and about 9 inches square section. Sides and ends were of glass and the base of slate. Two thin copper wires spaced 3 cm. apart were stretched inside parallel to its length, and the trough filled with liquid paraffin. On the top were arranged two sliding frames, one carrying a brass plate through which the wires passed and acting as a reflecting bridge, the other supporting a vacuum thermojunction detector close to the wires. At one end the wires were continued to form a loop loosely coupled to the magnetron anode circuit. The arrangement is shown diagramatically in fig. 10.

Results obtained with this apparatus fully confirmed those obtained by method A. They are given in the following table, ε being calculated from the relation $\lambda = \sqrt{\varepsilon}\,\lambda_\varepsilon$, where λ_ε is the wavelength measured in the dielectric.

Table 3.

λ (cm.)	λ_ε (cm.)	ε
21·64	14·61	2·20
24·00	16·14	2·21
24·08	16·23	2·20
24·18	16·32	2·20
24·26	16·40	2·19

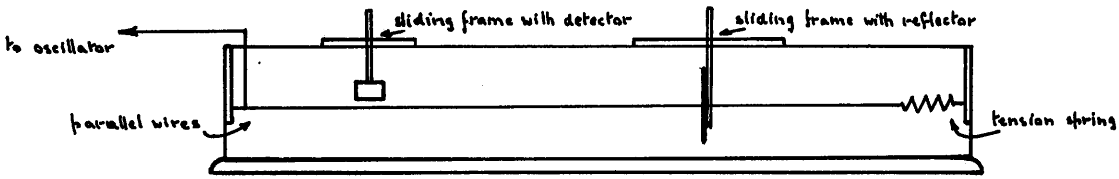

Fig. 10. Diagrammatic view of trough arrangement.

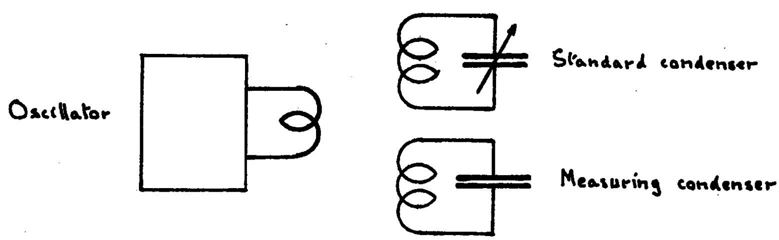

Fig. 11. Arrangement for low-frequency measurement.

λ (cm.)	λ_ε (cm.)	ε
24·30	16·50	2·17
24·40	16·40	2·21
24·56	16·50	2·21
24·68	16·68	2·19
27·71	18·70	2.20
	Mean	2·20

Liquid paraffin, if pure, is non-polar, and so its dielectric constant would be expected to remain practically constant from low frequencies to optical frequencies. Therefore, as further confirmation of the results, two such measurements were made, one at $\lambda = 45{\cdot}7$ m., and the other for sodium D light, $\lambda = 5893$ A.

For the radio-frequency measurement the arrangement shown in fig. 11 was used. The oscillator is tuned to the natural frequency of the circuit containing the measuring condenser, then the standard condenser circuit is also tuned to this frequency. The measuring condenser is now immersed in liquid paraffin and the oscillator and standard condenser circuit tuned to the new natural frequency. The dielectric constant is given by the ratio of the capacity of the measuring condenser in the two cases, which is equal to the ratio of the standard condenser readings. The value obtained was

$$\varepsilon = \frac{1219\,\mu\mu F.}{558\,\mu\mu F.} = 2{\cdot}18$$

with an accuracy of about 2 per cent.

The optical measurement was made with a spectrometer using a hollow prism filled with liquid paraffin. The result obtained was 2·20.

These results are all in good agreement. They will be discussed in a subsequent chapter when results by modified wave guide methods are available.

Chapter 3.

EXPERIMENTS WITH IONIZED AIR.

8. Ionosphere Studies.

In connection with ionosphere studies, use has been made of the formulae of Larmor, Lorentz and others on the propagation of electromagnetic waves in a space containing free electrons. For the longer wireless waves experimental investigations were made on reflection from the ionized layers of the upper atmosphere, but for wavelengths of the order of a metre or two it became possible to make experiments on a locally produced ionized space - "artificial ionosphere". The essence of these measurements is to find the dielectric constant and conductivity of the ionized space, and the experimental method adopted by Mitra and Banerjee[11] and others is to place a long discharge tube between the two wires of an excited Lecher wire system, a low pressure direct current discharge being maintained in it.

It was considered that the wave guide could with advantage replace the Lecher wires for investigation of ionization effects at very high frequencies, its merit again being the inclusion of the total field within the volume of the dielectric. However, a gas discharge to supply the electrons could not be produced to occupy the whole interior of the metal tube, and it was decided to use an ionizing agent in the tube. First of all a theoretical investigation was made which is given below, and this is followed by a description of the experimental procedure.

9. Propagation in a Wave Guide containing Free Electrons.

Appleton[12] has given the theory of propagation of plane waves in a space containing free electrons and in the presence of a superimposed magnetic field. The following investigation is based on his methods, but an external magnetic field is not considered.

Let us consider the case of a wave guide with its axis as the z-axis of coordinates. Let E, H, P, j be respectively the electric force, magnetic force, polarization, and convection-current density at any point. Maxwell's field equations in the tube, written in cylindrical polars, are

$$\left.\begin{aligned}
\frac{1}{c}\dot{E}_\rho + 4\pi j_\rho &= \frac{1}{\rho}\frac{\partial H_z}{\partial \varphi} - \frac{\partial H_\varphi}{\partial z} \\
\frac{1}{c}\dot{E}_\varphi + 4\pi j_\varphi &= \frac{\partial H_\rho}{\partial z} - \frac{\partial H_z}{\partial \rho} \\
\frac{1}{c}\dot{E}_z + 4\pi j_z &= \frac{1}{\rho}\left[\frac{\partial}{\partial \rho}(\rho H_\varphi) - \frac{\partial H_\rho}{\partial \varphi}\right] \\
-\frac{1}{c}\dot{H}_\rho &= \frac{1}{\rho}\frac{\partial E_z}{\partial \varphi} - \frac{\partial E_\varphi}{\partial z} \\
-\frac{1}{c}\dot{H}_\varphi &= \frac{\partial E_\rho}{\partial z} - \frac{\partial E_z}{\partial \rho} \\
-\frac{1}{c}\dot{H}_z &= \frac{1}{\rho}\left[\frac{\partial}{\partial \rho}(\rho E_\varphi) - \frac{\partial E_\rho}{\partial \varphi}\right]
\end{aligned}\right\} . \qquad (6)$$

For an angular frequency p and propagation constant β we introduce the exponential factor $e^{i(pt-\beta z)}$. The case of E-waves will be considered, and for these $H_z = 0$. As the E_0-wave would be used, the analysis can be simplified by introducing here the restrictions for zero order waves, viz: $E_\varphi = H_\rho = \frac{\partial}{\partial \varphi} = 0$. The equations now reduce to

$$\left.\begin{aligned}
E_\rho + 4\pi P_\rho &= \beta c/p\, H_\varphi \\
P_\varphi &= 0 \\
E_z + 4\pi P_z &= -\frac{ic}{p\rho}\frac{\partial}{\partial \rho}(\rho H_\varphi) \\
H_\varphi &= \frac{\beta c}{p}E_\rho - \frac{ic}{p}\frac{\partial E_z}{\partial \rho}
\end{aligned}\right\} . \qquad (7)$$

The motion of an electron subjected to a restoring force proportional to its displacement and a frictional force proportional to the velocity, is given by the equation

$$m\ddot{\underset{\sim}{r}} = e\left(\underset{\sim}{E} + \frac{4\pi}{3}\underset{\sim}{P}\right) - f\underset{\sim}{r} - g\dot{\underset{\sim}{r}} \;,$$

from which we get the Lorentz equation

$$4\pi \underset{\sim}{P} = \frac{\underset{\sim}{E}}{u + iv} \;, \tag{8}$$

in which $\quad u = \dfrac{-p^2 m + f - \dfrac{4\pi N e^2}{3}}{4\pi N e^2}$.

and $\quad v = \dfrac{pg}{4\pi N e^2}$,

N being the number of electrons per c.c. Substituting from (8) in (7) and eliminating E_ρ and H_φ we get the wave propagation equation

$$\frac{\partial^2 E_z}{\partial \rho^2} + \frac{1}{\rho}\frac{\partial E_z}{\partial \rho} + p^2/c^2\left[1 + \frac{1}{u+iv} - \frac{\beta^2 c^2}{p^2}\right]E_z = 0 \,, \tag{9}$$

of which the solution, continuous within the tube boundaries, is

$$E_z = A J_0\left(\frac{p\rho}{c}\sqrt{1 + \frac{1}{u+iv} - \frac{\beta^2 c^2}{p^2}}\right). \tag{10}$$

The propagation constant is determined by applying the boundary condition that $(E_z)_{\rho=a} = 0$. If k has a value such that ka is the first zero of $J_0(ka) = 0$, then

$$\mathcal{R}\left\{\frac{p}{c}\sqrt{1 + \frac{1}{u+iv} - \frac{\beta^2 c^2}{p^2}}\right\} = k \,,$$

whence $\quad \left(\dfrac{2\pi}{\lambda}\right)^2\left\{1 + \dfrac{u}{u^2+v^2} - \left(\dfrac{\lambda}{\lambda_t}\right)^2\right\} = k^2,$

since $\quad \mathcal{R}(\beta) = \dfrac{2\pi}{\lambda_t}$.

Reducing further we get

$$\frac{1}{\lambda_t} = \sqrt{\frac{1 + \frac{u}{u^2+v^2}}{\lambda^2} - \left(\frac{k}{2\pi}\right)^2} \;. \tag{11}$$

Comparing this with equation (3) we see that it corresponds to a dielectric constant

$$\varepsilon = 1 + \frac{u}{u^2+v^2}$$

$$= 1 - \frac{4\pi N e^2}{m p^2 + \frac{4\pi N e^2}{3}}, \qquad (12)$$

neglecting the frictional term, which is that deduced by Lorentz.

Putting λ_{t_0} for the tube wavelength with air as dielectric, then

$$\frac{1}{\lambda_t} \doteq \frac{1}{\lambda_{t_0}}\left\{1 + \frac{u}{2(u^2+v^2)}\left(\frac{\lambda_{t_0}}{\lambda}\right)^2\right\}. \qquad (13)$$

So, if a change of 5 per cent is assumed to be the least accurately determinable change in tube wavelength due to the electrons, then, approximately, $\frac{1}{2u}\left(\frac{\lambda_{t_0}}{\lambda}\right)^2 > \frac{1}{20}$.
Inserting typical values for λ = 20 cm. we find that $N > 2.10^8$. Thus to make useful measurements with the apparatus the number of electrons per c.c. must be of the order of 2.10^8 at least.

10. Experiments with Artificial Ionosphere in Wave Guide.
The method chosen of producing the ionization was by means of uranium oxide, by α-particle collision. A quantity of the black oxide U_2O_5 was mixed with paste and spread on a sheet of stiff paper. When dry this was bent into a cylinder which was slipped into the tube. All openings in the tube were closed and the joints sealed with vacuum wax. The bearing of the reflecting piston was sealed with "Q" compound so that movement of the piston was possible. A connection was provided to a rotary vacuum pump and by this means the pressure

in the tube was reduced to a few millimetres.

With an oscillator wavelength of about 20 cm. the distance between resonant positions of the piston was measured and hence the wavelength in the tube determined, but this was found not to differ sensibly from that calculated from equation (3) for a normal air dielectric. It was assumed that this was due to too small a concentration of electrons, although the actual concentration was not readily calculable. Values of N up to 10^9 have been employed by experimenters who used discharge tubes, and from the calculation in the previous section it would seem that a value nearly equal to this would be necessary here. It was not at all obvious how the electron concentration could be measured, or, alternatively, how it could be increased, and so, when this negative result had been obtained at several frequencies and for various pressures, the experiment was abandoned.

Chapter 4.

THEORY OF DIELECTRIC MEASUREMENTS.

11. Method of Measurement for Solid Dielectrics.

The method described in section 6 for the measurement of dielectric constant is suitable only for liquids, since, obviously, a probe cannot be moved inside a solid to find the positions of loops and nodes. Measurements have however been made by various experimenters, using a parallel wire system which for part of its length runs through a block of solid dielectric. Such a method seemed a suitable one for use with the wave guide, since a cylinder of dielectric material could easily be inserted in the tube.

Two procedures suggested themselves

(1) that a cylinder of dielectric be inserted in the tube and the remainder filled with a liquid of higher dielectric constant. From the critical wavelength for this arrangement the dielectric constant of the solid could be found,

(2) that a cylinder of dielectric be inserted in the tube, the remainder being air filled. From the displacement of the stationary wave pattern caused by inserting the dielectric it should be possible to calculate the dielectric constant.

Both these methods were tried and an account of them is given in the following sections.

12. Critical Wavelength Method for Solid Dielectrics.

It was proposed to have a short length of the tube filled with a solid dielectric and the rest of the tube on both sides filled up with a liquid. If the liquid is of greater dielectric constant than the solid then the cut-off wavelength for the solid will be less than that for the liquid, and so if a wave is generated at one end of the tube and a detector placed at the other, the wavelength of the generated wave can be increased until no response is indicated on the detector. This will determine the critical wavelength for the solid.

Water, having at these frequencies a dielectric constant of about 81, was considered suitable for the liquid, and so, as a prelude, the tube was filled with water. Tap water was used, and a generator wavelength of 20 cm., but no transmitted wave could be detected. It was thought that this would be due to absorption in the water, and so a length was cut from the tube in order that the detector could be taken up close to the source. Still no wave was detectable, nor was there any when the tap water was replaced by distilled water. In attempts to obtain greater sensitivity in the detecting device the thermojunction was replaced by a small zincite-bornite crystal detector and the Unipivot microammeter by a sensitive Broca galvanometer, but these provided only a small constant deflection. A positive result was, however, obtained at a wavelength of 160 cm., and from this a value of the dielectric constant of water of 84 was calculated. This wavelength is well above the critical value for most dielectrics for the diameter of tube used and is thus of no value. At wavelengths of 20 cm. the wavelength in water would be about 2 cm. and so the detector would indicate a maximum every centimetre. As this is quite comparable with the dimensions of the detector it is perhaps not surprising that no indication of stationary waves was found, although a readable constant deflection might have been expected. These negative results were confirmed by similar experiments using the glass trough previously described, this time filled with water. Positive indications were obtained only at wavelengths over a metre.

By reason of these difficulties the method was temporarily abandoned, and it was hoped that further investigations would be possible at a future date.

13. Displacement Method for Solid Dielectrics.

For application to the wave guide of the second method outlined in section 11 it was proposed to place a short cylinder of dielectric in the tube, where previously the reflector had been set to produce a stationary wave system. The introduction of the dielectric would require the reflector to be moved inwards to restore the stationary pattern, and from this movement the dielectric constant would be calculated.

Quite simple formulae had been used by others, but a theoretical investigation appeared to show that the wave guide case was more complex. During the investigation a paper by King[13] was found in which the parallel wire case was fully treated, but the physical implications of the mathematical results were not evident. A treatment starting from Maxwell's equations proved much more revealing than that of King, who had used the telegraphic equations. It also appeared that previous workers had made unjustifiable assumptions.

This theory is given below, and is followed by a similar treatment for the wave guide. There is a definite advantage in giving here the parallel wire case as the underlying principles can be developed more easily for it, and it can then be shown how these are modified in the wave guide case.

14. Parallel Wire Line with Discontinuous Dielectric.

14.1. Resonance Condition.

The two systems represented in Fig. 12 will be analysed.

(1) represents a parallel wire system in air coupled at one end to a high-frequency oscillator and closed at the other by a movable bridge so placed that the system is in resonance.

(2) shows the same system with a section of the wires surrounded by a dielectric contained between planes perpendicular to the wires and supposedly infinite in extent. The frequency of the oscillator being constant, the bridge must obviously be moved to restore resonance.

Let an arbitrary origin be taken at O, and let z_1, z_2 be the abscissae of the dielectric faces, and z_3, z_4 the abscissae of the bridge positions in (2) and (1).

Let zone 0 extend from $z = 0$ to $z = z_1$

zone 1 extend from $z = z_1$ to $z = z_2$

zone 2 extend from $z = z_2$ to $z = z_3$

The propagation constant in zones 0 and 2 is β, and in zone 1 is β_1, these being equal to $2\pi/\lambda$ and $2\pi/\lambda_1$ res-

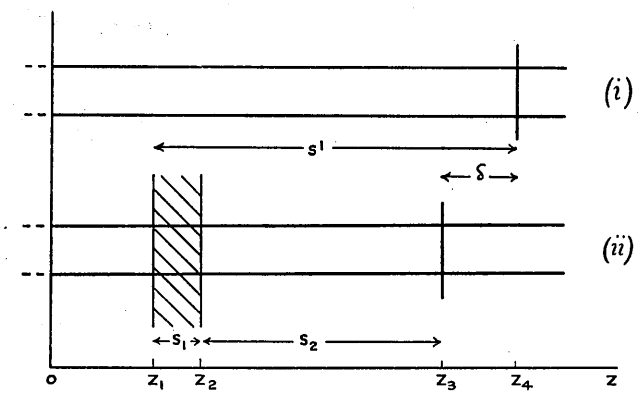

Fig. 12.

pectively. Solutions of the wave propagation equations for an angular frequency p give for the electric and magnetic intensities of a plane wave in Gaussian units

$$E = Ae^{i(pt-\beta z)} + Be^{i(pt+\beta z)},$$
$$H = \frac{c\beta}{p}\left\{Ae^{i(pt-\beta z)} - Be^{i(pt+\beta z)}\right\},$$

where c is the velocity of light. The first term is a wave progressing in the direction of z, and the second a wave in the direction of $-z$. A factor expressing the distribution in the (x,y) plane has been omitted as it plays no part in the succeeding work. The permeability factor μ is also omitted throughout, being assumed to be unity.

The same equations hold for the coaxial cable.

Denoting the above zones by subscripts, we get

$$\left.\begin{aligned} E_0 &= A_0e^{i(pt-\beta z)} + B_0e^{i(pt+\beta z)}, \\ E_1 &= A_1e^{i(pt-\beta_1 z)} + B_1e^{i(pt+\beta_1 z)}, \\ E_2 &= A_2e^{i(pt-\beta z)} + B_2e^{i(pt+\beta z)}, \\ H_0 &= \frac{c\beta}{p}\left\{A_0e^{i(pt-\beta z)} - B_0e^{i(pt+\beta z)}\right\}, \\ H_1 &= \frac{c\beta_1}{p}\left\{A_1e^{i(pt-\beta_1 z)} - B_1e^{i(pt-\beta_1 z)}\right\}, \\ H_2 &= \frac{c\beta}{p}\left\{A_2e^{i(pt-\beta z)} - B_2e^{i(pt-\beta z)}\right\}. \end{aligned}\right\} \quad \ldots\ldots\ldots\ldots\ldots(14)$$

The boundary conditions at z_1 and z_2 require that E and H (which are, of course, in the (x,y) plane) should be continuous, i.e.,

$$\left.\begin{aligned} A_0e^{-i\beta z_1} + B_0e^{i\beta z_1} &= A_1e^{-i\beta_1 z_1} + B_1e^{i\beta_1 z_1}, \\ A_1e^{-i\beta_1 z_2} + B_1e^{i\beta_1 z_2} &= A_2e^{-i\beta z_2} + B_2e^{i\beta z_2}, \\ A_0e^{-i\beta z_1} - B_0e^{i\beta z_1} &= n\left(A_1e^{-i\beta_1 z_1} - B_1e^{i\beta_1 z_1}\right), \\ n\left(A_1e^{-i\beta_1 z_2} - B_1e^{i\beta_1 z_2}\right) &= A_2e^{-i\beta z_2} - B_2e^{i\beta z_2}, \end{aligned}\right\} \quad \ldots\ldots\ldots\ldots(15)$$

where $$n = \frac{c\beta_1}{p}\Big/\frac{c\beta}{p} = \frac{\beta_1}{\beta} = \sqrt{\varepsilon}\,, \quad \ldots\ldots\ldots\ldots\ldots\ldots(16)$$

and is here the index of refraction of the medium. The substitutions $n = \sqrt{\varepsilon}$ and $\beta_1 = \sqrt{\varepsilon}\beta$ are not made at present in order to allow comparison with the results in section 16, where these relations do not hold.

At the bridge end of the system, for perfect reflection

$$A_2 e^{-i\beta z_3} + B_2 e^{+i\beta z_3} = 0. \qquad \text{.............(17)}$$

If we now choose O such that the incident and reflected waves in case (2) produce a node of electric intensity at O, then

$$A_0 + B_0 = 0. \qquad \text{.............(18)}$$

Equations (15) and (18) now define the six constants in terms of any one of them. Solving in terms of A_0 we get

$$\left.\begin{aligned} A_1 &= \tfrac{1}{2} A_0 e^{i\beta_1 z_1}\left\{\left(1+\tfrac{1}{n}\right)e^{-i\beta z_1} - \left(1-\tfrac{1}{n}\right)e^{i\beta z_1}\right\}, \\ B_1 &= \tfrac{1}{2} A_0 e^{-i\beta_1 z_1}\left\{\left(1-\tfrac{1}{n}\right)e^{-i\beta z_1} - \left(1+\tfrac{1}{n}\right)e^{i\beta z_1}\right\}, \end{aligned}\right\} \text{.............(19)}$$

$$\left.\begin{aligned} A_2 = \tfrac{1}{4} A_0 e^{i\beta z_2}\Big[&(1+n)e^{-i\beta_1 z_2}\left\{\left(1+\tfrac{1}{n}\right)e^{i(\beta_1-\beta)z_1} - \left(1-\tfrac{1}{n}\right)e^{i(\beta_1+\beta)z_1}\right\} \\ &+ (1-n)e^{i\beta_1 z_2}\left\{\left(1-\tfrac{1}{n}\right)e^{-i(\beta_1+\beta)z_1} - \left(1+\tfrac{1}{n}\right)e^{-i(\beta_1-\beta)z_1}\right\}\Big], \\ B_2 = \tfrac{1}{4} A_0 e^{-i\beta z_2}\Big[&(1-n)e^{-i\beta_1 z_2}\left\{\left(1+\tfrac{1}{n}\right)e^{i(\beta_1-\beta)z_1} - \left(1-\tfrac{1}{n}\right)e^{i(\beta_1+\beta)z_1}\right\} \\ &+ (1+n)e^{i\beta_1 z_2}\left\{\left(1-\tfrac{1}{n}\right)e^{-i(\beta_1+\beta)z_1} - \left(1+\tfrac{1}{n}\right)e^{-i(\beta_1-\beta)z_1}\right\}\Big]. \end{aligned}\right\} \text{...(20)}$$

Substituting in (17) and reducing, we get the eliminant

$$n \cot\beta_1 s_1 \left(\cot\beta z_1 + \cot\beta s_2\right) + \cot\beta z_1 \cot\beta s_2 - n^2 = 0. \text{............(21)}$$

where $z_2 - z_1$ and $z_3 - z_2$ have been replaced by s_1 and s_2 respectively. The factor $\sin\beta_1 s_1 \sin\beta z_1 \sin\beta s_2$, which has been omitted from (21) for convenience, disposes of singularities. This equation expresses s_2 as a periodic function of z_1, and shows that the reduction in resonant length produced by the dielectric slab is a function of the absolute position of the slab. The result is somewhat unexpected, as a shift equal to the "optical path difference" between the dielectric and an equal thickness of air would seem plausible, and has indeed been assumed by some authors. It must be remembered, however, that in the optical problems where such a result is true the interference is between two separate travelling waves. Here the interference is between an incident wave and the fractions of it reflected at z_1, z_2 and z_3.

For case (1), since 0 and z_4 are nodes, $\beta z_4 = \nu\pi$ where ν is an integer, and, if $z_1 + s' = z_4 = \frac{\nu\pi}{\beta}$ defines s', (21) can be rewritten

$$n \cot\beta_1 s_1 \left(\cot\beta s' - \cot\beta s_2\right) + \cot\beta s' \cot\beta s_2 + n^2 = 0 \qquad (22)$$

This is the equation which King(13) has derived* . He has used the admittance expressions of the theory of the transmission line, which, although producing equation (22) more simply than the above, throw no light on the cause of the variation in resonant length with dielectric position, or the distribution of resultant amplitude and phase along the line. The various relations derived above enable these problems to be studied.

* With the exception that King has introduced a term expressive of the effect of a thin retaining wall on the faces of the dielectric.

If δ is the shift of the bridge required to restore resonance after the insertion of the dielectric, s_2 can be replaced by $s'-(s_1+\delta)$. The graph of δ against s' as given by (22) with this modification is of the form shown in fig. 13.

It can be shown by differentiation that the abscissæ of the turning points of this curve are given by

$$\tan \beta s' = \frac{1}{n} \tan \tfrac{1}{2}\beta_1 s_1 \qquad (23)$$

and

$$\tan \beta s' = -\frac{1}{n} \cot \tfrac{1}{2}\beta_1 s_1, \qquad (24)$$

and the corresponding values of δ by

$$\tan \tfrac{1}{2}\beta(s_1+\delta) = \frac{1}{n} \tan \tfrac{1}{2}\beta_1 s_1 , \qquad (25)$$

$$\tan \tfrac{1}{2}\beta(s_1+\delta) = n \tan \tfrac{1}{2}\beta_1 s_1 . \qquad (26)$$

Which of equations (25) and (26) represents δ_{max} and which δ_{min} depends on the sign of tan $\frac{1}{2}\beta_1 s_1$, i.e. upon the thickness s_1 of the slab. Since $n>1$, it is evident that, when $\left[\frac{2s_1}{\lambda_1}\right]$* is zero or an even integer, (25) gives δ_{min} and (26) δ_{max} ; for $\left[\frac{2s_1}{\lambda_1}\right]$ an odd integer (25) gives δ_{max} and (26) δ_{min}.†

From (23) and (25)

$$\tan \beta s' = \tan \tfrac{1}{2}\beta(s_1+\delta) = \tan \tfrac{1}{2}\beta(s'-s_2),$$

$$\therefore \quad \beta s' = \tfrac{1}{2}\beta(s'-s_2) + \nu\pi$$

i.e.,

$$s' + s_2 = \nu\lambda,$$

* $[x]$ denotes the integral part of x.

† King states without qualification that his equation (14), corresponding to (25) here, represents a maximum. This is, of course, true for his experimental values.

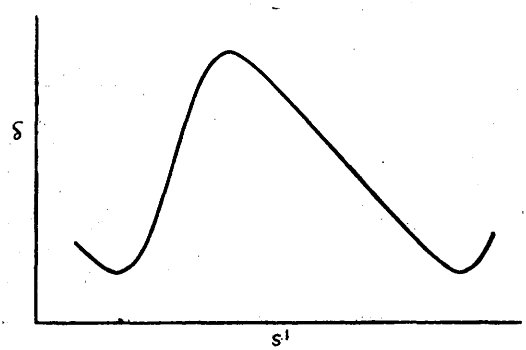

Fig. 13. General form of shift curve.

or, assuming z_1 and s_2 to be the distances of the first nodes from either side of the dielectric, $s_2 = z_1$.
Similarly from (24) and (26) $s' + s_2 = (\nu + \frac{1}{2})\lambda$; in particular $s_2 = z_1$.

These results show that for maximum and minimum shift the dielectric slab is so placed that nodes on both sides are symmetrical with respect to the slab.

14.2. <u>Boundary Effects in a System obeying the Resonance Condition.</u>

Using equations (14), (18), (19), (20), the following expressions are obtained for E_0, E_1 and E_2 :

$$E_0 = -2A_0 i e^{ipt} \sin\beta z, \quad 0 \leq z \leq z_1, \tag{27}$$

$$\begin{aligned} E_1 &= -2A_0 i e^{ipt}\left(\cos\beta_1 s \sin\beta z_1 + \frac{1}{n}\sin\beta_1 s \cos\beta z_1\right) \\ &= -2A_0 i e^{ipt}\sqrt{\sin^2\beta z_1 + \frac{1}{n^2}\cos^2\beta z_1}\,.\,\sin\left\{\beta_1 s + \tan^{-1}(n\tan\beta z_1)\right\}, \end{aligned} \tag{28}$$

$$0 \leq s \leq z_2 - z_1,$$

where $s = z - z_1$,

$$\begin{aligned} E_2 &= -2A_0 i e^{ipt}\frac{1}{n}\Big\{\sin\beta s''\left(n\cos\beta z_1 \cos\beta_1 s_1 - n^2 \sin\beta z_1 \sin\beta_1 s_1\right) \\ &\qquad + \cos\beta s''\left(\cos\beta z_1 \sin\beta_1 s_1 + n\sin\beta z_1 \cos\beta_1 s_1\right)\Big\} \\ &= -2A_0 i e^{ipt} R \sin(\beta s'' + \varphi), \quad 0 \leq s'' \leq z_3 - z_2, \end{aligned} \tag{29}$$

where

$$R = \left\{\left(\cos\beta z_1 \cos\beta_1 s_1 - n\sin\beta z_1 \sin\beta_1 s_1\right)^2 + \left(\frac{1}{n}\cos\beta z_1 \sin\beta_1 s_1 + \sin\beta z_1 \cos\beta_1 s_1\right)^2\right\}^{\frac{1}{2}}$$

$$\tan\varphi = \frac{\frac{1}{n}\tan\beta_1 s_1 + \tan\beta z_1}{1 - n\tan\beta_1 s_1 \tan\beta z_1}$$

and $s'' = z - z_2$.

Before reduction E_1 and E_2 are observed to consist of four waves, two travelling in the z direction and two in the $-z$ direction. The expressions given are the stationary waves which are the resultants of these components.

At $z = z_1$ $E_0 = -2A_0 i e^{ipt} \sin\beta z_1$,

at $s = 0$ $E_1 = -2A_0 i e^{ipt} \sin\beta z_1$.

At the boundary therefore E_0 and E_1 have the same intensity, but the phases are not equal, being respectively βz_1 and $\tan^{-1}(n \tan\beta z_1)$. It is easy to show, remembering the relation $\beta_1 = \sqrt{\varepsilon}\beta$, that

$$\left(\frac{\partial E_0}{\partial z}\right)_{z=z_1} = \left(\frac{\partial E_1}{\partial s}\right)_{s=0}. \tag{30}$$

Similar results can be shown to hold for the second boundary.

Thus, although for any progressive train of waves crossing a boundary of dielectrics there will be a change of intensity by reflexion and no change of phase between incident and transmitted beam, in this case for the condition of resonance the reflexions at the bridge and at dielectric boundaries are such that the resultant stationary wave shows no change of intensity at the boundary *, but does show a phase change. From the above results it is seen that the magnitude of the phase change is dependent upon z_1, i.e., upon the position of the dielectric relative to the original standing wave system. In this lies the explanation of the variation of bridge shift with dielectric position. From (30) we see that the phase change at a boundary is always such as to make the gradient of electric intensity continuous. Fig. 14

* This does not mean that the amplitudes of E_0, E_1, E_2 are equal.

illustrates these conditions; the curves represent extreme values of E .

The expressions for the magnetic field, viz.,

$$\left.\begin{aligned} H_0 &= 2A_0 e^{ipt} \cos\beta z, \\ H_1 &= 2A_0 e^{ipt} \sqrt{\varepsilon} \sqrt{\sin^2\beta z_1 + \tfrac{1}{n^2}\cos^2\beta z_1}\,.\cos\{\beta_1 s + \tan^{-1}(n\tan\beta z_1)\} \\ H_2 &= 2A_0 e^{ipt} R \cos(\beta s'' + \varphi), \end{aligned}\right\} \quad (31)$$

are similar to those of the electric field displaced by $\pi/2$, with the exception that a factor $\sqrt{\varepsilon}$ appears in H_1 (this factor is present, equal to unity, in H_0 and H_2 .) The gradient of H is now discontinuous at a boundary (except when zero). The relative amplitudes of E and H follow the usual law for propagation of plane waves, viz., $H = \sqrt{\varepsilon}\,E$, and the discontinuity of gradient is such that loops of H are coincident with nodes of E.

As the potential between the wires is obtained by a line integration of the complete expression for the electric force, potential distribution is the same as distribution of E ; current in the wires, being an integral of magnetic force, follows the distribution of H.

A decrease δ in the resonant length of the line is due to a phase increase of $\beta\delta$ in both E and H. This total phase increase will be due to:

2 phase shifts at dielectric boundaries $+$ phase increase due to optical path difference between dielectric and the

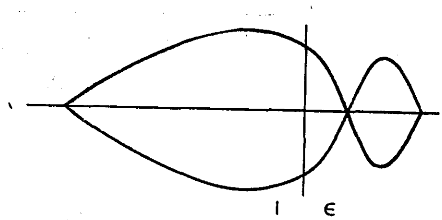

Fig. 14.

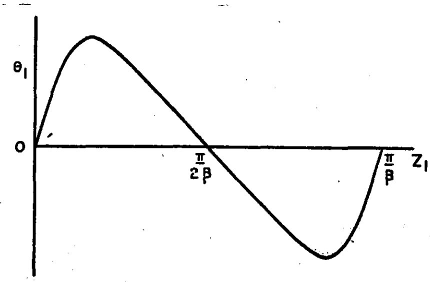

Fig. 15.

same thickness of air.

This can be expressed as

$$\beta\delta = \theta_1 + \theta_2 + (\beta_1 - \beta)s_1 .$$

From (27), (28), (29),

$$\theta_1 = \tan^{-1}(n \tan\beta z_1) - \beta z_1 , \qquad \text{.............(32)}$$

$$\theta_2 = \tan^{-1}\left\{\frac{\frac{1}{n}\tan\beta_1 s_1 + \tan\beta z_1}{1 - n\tan\beta z_1 \tan\beta_1 s_1}\right\} - \tan^{-1}(n\tan\beta z_1) - \beta_1 s_1 . \qquad \text{.............(33)}$$

The relation between θ_1 and z_1, for $n = 4$, is shown graphically in fig. 15. From it we see that if $0 < z_1 < \frac{1}{4}\lambda$ there will be an advance of phase at the boundary, and a retardation for $\frac{1}{4}\lambda < z_1 < \frac{1}{2}\lambda$. Turning points on the curve are given by

$$\tan\beta z_1 = \pm\frac{1}{\sqrt{n}} ,$$

and so the skewness increases with n.

If we replace $\tan\beta z_1$ by its value in terms of s_1 and s_2 given by (21) we obtain

$$\theta_2 = \tan^{-1}(n\tan\beta s_2) - \beta s_2$$

which is of the same form as θ_1. For the conditions of

δ_{max} and δ_{min} $\qquad \theta_1 = \theta_2 ,$

and since also $z_1 = s_2$ for these cases, we see from fig. 15 that,

if $\qquad 0 < z_1 = s_2 < \frac{1}{4}\lambda ,$

δ will be a maximum;

if $\qquad \frac{1}{4}\lambda < z_1 = s_2 < \frac{1}{2}\lambda ,$

δ will be a minimum.

The phase change due to the optical path difference is, for δ_{max}, increased by two equal boundary shifts, and, for δ_{min}, decreased by two equal boundary shifts.

14.3. Relative Amplitudes.

$$|E_0| = 2A_0$$
$$|E_1| = 2A_0\sqrt{\sin^2\beta z_1 + \tfrac{1}{n^2}\cos^2\beta z_1}$$
$$|E_2| = 2A_0\left\{\left(\cos\beta z_1\cos\beta_1 s_1 - n\sin\beta z_1\sin\beta_1 s_1\right)^2 + \left(\tfrac{1}{n}\cos\beta z_1\sin\beta_1 s_1 + \sin\beta z_1\cos\beta_1 s_1\right)^2\right\}^{\frac{1}{2}}.$$

It can be seen that $|E_1|$ varies between the limits $|E_0|$ and $\frac{1}{\sqrt{\varepsilon}}|E_0|$, and $|E_2|$ between limits $\sqrt{\varepsilon}|E_0|$ and $\frac{1}{\sqrt{\varepsilon}}|E_0|$. This is also the potential distribution. The limits for the magnetic field, and hence current, are

$$|H_0| \leqslant |H_1| \leqslant \sqrt{\varepsilon}\,|H_0|,$$
$$\frac{1}{\sqrt{\varepsilon}}|H_0| \leqslant |H_2| \leqslant \sqrt{\varepsilon}\,|H_0|.$$

14.4. Summary.

It has been shown that, on surrounding part of the length of a Lecher wire system by a dielectric, a decrease in the resonant length is produced, which is dependent on the position of the dielectric slab. For a system in resonance the following are true:

(1) At a dielectric boundary the electric and magnetic intensities are continuous.

(2) A phase change is produced the same in both electric and magnetic components and such that the gradient of electric intensity is continuous. Loops of magnetic force coincide with nodes of electric force.

(3) The amplitudes of the stationary waves in the three zones are in general different and vary relatively between definite limits. The typical general case of fig. 16

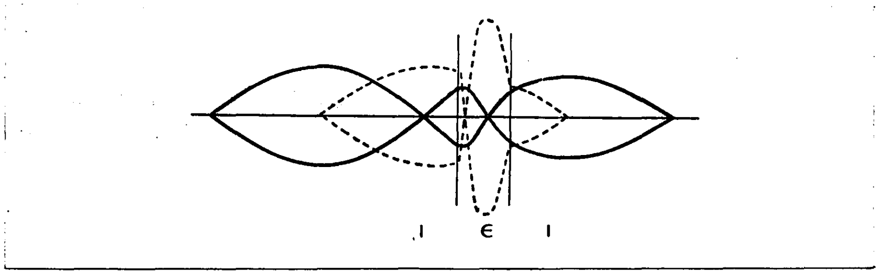

Fig. 16.

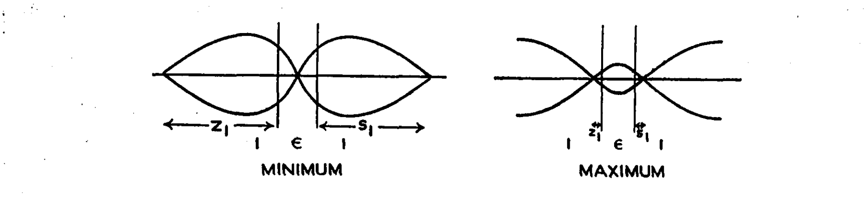

Fig. 17.

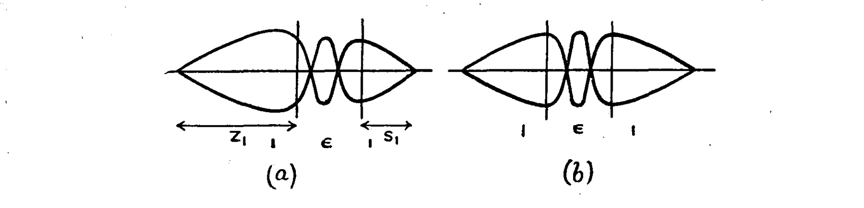

Fig. 18.

illustrates these results, solid lines being of electric intensity and dotted lines of magnetic intensity.

(4) For maximum and minimum bridge displacement the wave distribution is symmetrical with respect to the dielectric slab. Examples of this are shown in fig. 17.

14.5. Particular Cases.

An interesting particular case, fig. 18 (a), is where s_1 is a whole number of dielectric half-wave-lengths. Then $\theta_1 + \theta_2 = 0$, and δ depends only on the optical path difference, and is therefore constant for all positions of the slab. In this case the part s_1 of the wave is the complement of the part z_1.

When a node or a loop coincides with a dielectric boundary the phase change there is zero. When a loop coincides with the boundary the amplitudes on both sides of it are equal. Fig. 18 (b) illustrates this as a particular case of 18 (a): all three amplitudes are here equal.

15. Previous Investigations.

A number of investigators have employed experimental arrangements similar to that considered here, without fully appreciating the principles involved.

Smith-Rose and McPetrie[14], in an investigation on the dielectric constant of soil, used a box of soil with two parallel wires passing through it. One end was made to coincide with a voltage node, "so that the effect of reflexion at the boundary between soil and air would be reduced to a minimum"; the other end, however, did not coincide with a node or loop (except perhaps fortuitously). The formula stated was the result of equating bridge shift to optical path difference. Neglect of the second boundary effect invalidates this formula and the results obtained.

The results of Banerjee and Joshi[15], who used the same formula in a similar investigation, are also in error.

Seeberger[16] was puzzled by the variation of bridge shift with dielectric position, and dismissed it as "unübersichtlich."

Hormell[17] alone seems to have appreciated the boundary effect, although he does not say so explicitly. In a measurement of the dielectric constant of paraffin wax he cut the slab until each end coincided with a current loop (thus making θ_1 and θ_2 zero).

16. Wave Guide with Discontinuous Dielectric.

16.1. H-waves.

The expressions for E and H for an H-wave in a wave guide are given in cylindrical coordinates ρ, φ, z by[3]

$$\left.\begin{aligned}
H_z &= J_\nu(k\rho)\cos\nu\varphi\left(Ae^{i(pt-\beta z)} + Be^{i(pt+\beta z)}\right),\\
E_z &= 0,\\
E_\rho &= \frac{\nu p}{ik^2\rho c} J_\nu(k\rho)\sin\nu\varphi\left(Ae^{i(pt-\beta z)} + Be^{i(pt+\beta z)}\right),\\
E_\varphi &= -\frac{p}{ikc} J_\nu'(k\rho)\cos\nu\varphi\left(Ae^{i(pt-\beta z)} + Be^{i(pt+\beta z)}\right),\\
H_\rho &= \frac{\beta}{ik} J_\nu'(k\rho)\cos\nu\varphi\left(Ae^{i(pt-\beta z)} - Be^{i(pt+\beta z)}\right),\\
H_\varphi &= -\frac{\nu\beta}{ik^2\rho} J_\nu(k\rho)\sin\nu\varphi\left(Ae^{i(pt-\beta z)} - Be^{i(pt+\beta z)}\right).
\end{aligned}\right\} \quad (34)$$

k in the above equations has a value given by

$$J_\nu'(ka) = 0$$

and

$$\beta \equiv \frac{2\pi}{\lambda_{tube}} = 2\pi\sqrt{\frac{\epsilon}{\lambda^2} - \left(\frac{k}{2\pi}\right)^2}.$$

Let us take a tube, part of which between two diametral planes is filled with dielectric, the rest being filled with air, and let us define zones 0, 1, 2 as in Section 14.1. The air-dielectric boundary conditions are continuity of the tangential components $E_\rho, E_\varphi, H_\rho, H_\varphi$; for H_z which is perpendicular to the boundary plane, the condition is continuity of magnetic induction, but since permeability is assumed unity in both air and dielectric this reduces to continuity of H_z. The application of these conditions gives for H_z, E_ρ, E_φ

$$A_0 e^{-i\beta z_1} + B_0 e^{i\beta z_1} = A_1 e^{-i\beta_1 z_1} + B_1 e^{i\beta_1 z_1},$$
$$A_1 e^{-i\beta_1 z_2} + B_1 e^{i\beta_1 z_2} = A_2 e^{-i\beta z_2} + B_2 e^{i\beta z_2},$$

and for H_ρ, H_φ

$$\beta\left(A_0 e^{-i\beta z_1} - B_0 e^{i\beta z_1}\right) = \beta_1\left(A_1 e^{-i\beta_1 z_1} - B_1 e^{i\beta_1 z_1}\right),$$
$$\beta_1\left(A_1 e^{-i\beta_1 z_2} - B_1 e^{i\beta_1 z_2}\right) = \beta\left(A_2 e^{-i\beta z_2} - B_2 e^{i\beta z_2}\right).$$

These are formally identical with equations (15); n has the value β_1/β and hence now

$$n = \sqrt{\frac{\varepsilon - (k\lambda/2\pi)^2}{1 - (k\lambda/2\pi)^2}} \cdot \qquad (\text{cf.}\ (16)) \quad \ldots\ldots\ldots\ldots\ldots(35)$$

If the end of the tube is closed by a plane reflector, (17) will express this terminal condition. Now choose the origin of coordinates such that (18) is also satisfied. Since equations (15), (17), (18) all hold for the wave guide, the fundamental equation

$$n \cot\beta_1 s_1 \left(\cot\beta s' - \cot\beta s_2\right) + \cot\beta s' \cot\beta s_2 + n^2 = 0 \quad \ldots\ldots\ldots\ldots\ldots(22)$$

will also hold. It will give a shift curve with maxima and minima given as before by (23) to (26). Since n, β and β_1 have assumed new values the consequences of (22) may differ from those obtained in Section 14.

An obvious difference is that, whereas in Section 14.1 n was constant equal to $\sqrt{\varepsilon}$, now n given by (34) is a function of ε and of λ. Since to allow of transmission both numerator and denominator of (35) must be real, λ is restricted to values $< 2\pi/k$. The portion marked H in fig. 19 shows the mode of variation of n with λ in the permissible range. It increases from a value $\sqrt{\varepsilon}$ for infinitely high frequencies to an infinite value at the cut-off point.

It is obvious from comparison with the expressions for the components of E and H in Section 14.2 that the following results will hold (omitting nonsignificant factors):-

$$H_{z0} \sim E_{\rho 0} \sim E_{\varphi 0} \sim \sin\beta z,$$

$$H_{\rho 0} \sim H_{\varphi 0} \sim \beta\cos\beta z,$$

$$H_{z1} \sim E_{\rho 1} \sim E_{\varphi 1} \sim \sqrt{\sin^2\beta z_1 + \frac{1}{n^2}\cos^2\beta z_1}\,.\,\sin\left\{\beta_1 s + \tan^{-1}(n\tan\beta z_1)\right\},$$

$$H_{\rho 1} \sim H_{\varphi 1} \sim \beta_1\sqrt{\sin^2\beta z_1 + \frac{1}{n^2}\cos^2\beta z_1}\,.\,\cos\left\{\beta_1 s + \tan^{-1}(n\tan\beta z_1)\right\},$$

etc.

Once again, in addition to continuity of intensity at a boundary, we have an adjustment of relative amplitudes such that the electric field gradient (and also the gradient of H_z) is continuous.

With the appropriate changes the results of Section 14 are applicable, and similar distribution diagrams can be drawn.

16.2. <u>E-waves</u>.

For the case of a wave whose magnetic vector is wholly

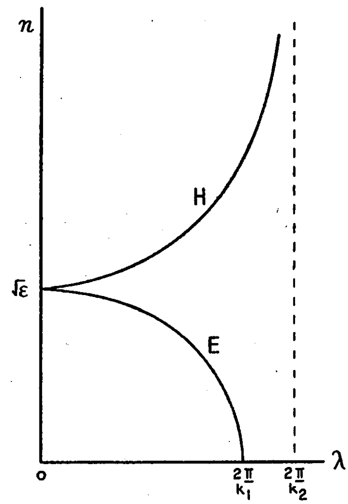

Fig. 19.

transverse the propagation equations in the wave guide are[3]

$$\left.\begin{aligned}
E_z &= J_\nu(k\rho)\cos\nu\varphi\left(A'e^{i(pt-\beta z)} - B'e^{i(pt+\beta z)}\right),\\
H_z &= 0,\\
E_\rho &= \frac{\beta}{ik}J_\nu'(k\rho)\cos\nu\varphi\left(A'e^{i(pt-\beta z)} + B'e^{i(pt+\beta z)}\right),\\
E_\varphi &= -\frac{\nu\beta}{ik^2\rho}J_\nu(k\rho)\sin\nu\varphi\left(A'e^{i(pt-\beta z)} + B'e^{i(pt+\beta z)}\right),\\
H_\rho &= \frac{p\nu\varepsilon}{ik^2\rho c}J_\nu(k\rho)\sin\nu\varphi\left(A'e^{i(pt-\beta z)} - B'e^{i(pt+\beta z)}\right),\\
H_\varphi &= \frac{p\varepsilon}{ikc}J_\nu'(k\rho)\cos\nu\varphi\left(A'e^{i(pt-\beta z)} - B'e^{i(pt+\beta z)}\right).
\end{aligned}\right\}\quad(36)$$

k in these equations has a value given by $J_\nu(ka) = 0$ and the propagation constant

$$\beta \equiv \frac{2\pi}{\lambda_{tube}} = 2\pi\sqrt{\frac{\varepsilon}{\lambda^2} - \left(\frac{k}{2\pi}\right)^2}.$$

For the interior of the tube divided into zones as before the air-dielectric boundary conditions are continuity of the tangential components; for E_z the condition is continuity of displacement. The application of these conditions gives for E_ρ and E_φ

$$\begin{aligned}
\beta\left(A_0'e^{-i\beta z_1} + B_0'e^{i\beta z_1}\right) &= \beta_1\left(A_1'e^{-i\beta_1 z_1} + B_1'e^{i\beta_1 z_1}\right),\\
\beta_1\left(A_1'e^{-i\beta_1 z_2} + B_1'e^{i\beta_1 z_2}\right) &= \beta\left(A_2'e^{-i\beta z_2} + B_2'e^{i\beta z_2}\right),
\end{aligned}$$

and for E_z, H_ρ, H_φ

$$\begin{aligned}
A_0'e^{-i\beta z_1} - B_0'e^{i\beta z_1} &= \varepsilon\left(A_1'e^{-i\beta_1 z_1} - B_1'e^{i\beta_1 z_1}\right),\\
\varepsilon\left(A_1'e^{-i\beta_1 z_2} - B_1'e^{i\beta_1 z_2}\right) &= A_2'e^{-i\beta z_2} - B_2'e^{i\beta z_2}.
\end{aligned}$$

If in these equations we put

$$\beta A_0' = A_0,\quad \beta_1 A_1' = A_1,\quad \beta A_2' = A_2,$$

and similar values for the B's, they reduce to equations (15) formally.

This time n has the value $\frac{\varepsilon\beta}{\beta_1}$, and hence

$$n = \varepsilon \sqrt{\frac{1-(k\lambda/2\pi)^2}{\varepsilon-(k\lambda/2\pi)^2}} \,. \qquad (37)$$

Applying as before the terminal and origin conditions (17) and (18), we get again the resonance relation (22)*.

* Schelkunoff[18] has shown that the differential equations of wave motion for E-waves can be expressed as

$$\partial V/\partial z = \left(\frac{ip}{c} + \frac{k^2c}{ip\varepsilon}\right)A = -ZA,$$
$$\partial A/\partial z = -\frac{ip\varepsilon}{c}V = -YV,$$

where V is a scalar potential function such that the transverse electric field $E_t = -\mathrm{grad}_t V$, and A is a vector parallel to the z-axis such that $H = \mathrm{curl}\, A$ and proportional to the longitudinal displacement current. These correspond exactly to the differential equations for current and potential in parallel wire or coaxial transmission lines, Z being the distributed series impedance and Y the distributed shunt admittance. We can therefore define the parameter $\sqrt{Z/Y}$ as the "characteristic impedance" of the tube. King[13] defines n in (22) as the ratio of the characteristic impedances of a parallel wire system in air and in the dielectric. Adapting this definition of n, and using the above expression for the characteristic impedance, we get

$$n = \sqrt{\frac{\frac{ip}{c}+\frac{k^2c}{ip}}{\frac{ip}{c}} \cdot \frac{\frac{ip\varepsilon}{c}}{\frac{ip}{c}+\frac{k^2c}{ip\varepsilon}}} \,,$$

which reduces to

$$\varepsilon \sqrt{\frac{1-(k\lambda/2\pi)^2}{\varepsilon-(k\lambda/2\pi)^2}} \,,$$

the expression found in (37).

For H-waves equation (35) can be similarly obtained by using Schelkunoff's values of

$$Z = \frac{ip}{c}, \quad Y = \frac{ip\varepsilon}{c} + \frac{k^2c}{ip} \,.$$

Again n is a function of λ varying this time in the range $\sqrt{\varepsilon}$ to 0, as shown in the curve marked E of fig. 19.

In particular, for any value of ε by appropriate choice of λ, n can be made unity. Substituting this value in (22), and reducing, we find

$$\begin{aligned} \cot \beta_1 s_1 &= \cot \beta (s' - s_2) \\ &= \cot \beta (s_1 + \delta) \end{aligned}$$

or

$$\beta_1 s_1 = \beta (s_1 + \delta). \qquad (38)$$

Thus the shift curve of fig. 13 has degenerated to a straight line, the shift being now constant and independent of the dielectric position. The value of λ for which $n = 1$ is given by

$$\begin{aligned} \lambda &= \frac{2\pi}{k}\sqrt{\frac{\varepsilon}{\varepsilon + 1}} \\ &= \lambda_c \sqrt{\frac{\varepsilon}{\varepsilon + 1}}, \end{aligned} \qquad (39)$$

where λ_c is the critical wave-length for the particular wave-type employed. If this point is found an easy means of determining ε is thus available.

For values of $n > 1$ the conditions for δ_{max} and δ_{min} will hold as in Section 14.1, but if $n < 1$ these conditions will be reversed, e.g., for $[2s_1/\lambda_1]$ odd

if $n > 1$, δ_{max} is given by (25);

if $n < 1$, δ_{max} is given by (26).

If we let δ_1 be the value of δ given by (26), and δ_2 the value given by (25), then

$$\delta_1 - \delta_2 = \frac{2}{\beta} \tan^{-1} \left\{ \frac{1}{2} \left(n - \frac{1}{n} \right) \sin \beta_1 s_1 \right\}. \qquad (40)$$

Fig. 20 shows the variation of this expression with λ, $\delta_1 - \delta_2$

being expressed in units of wave-length. The zero nearest to λ_c is the point where $n = 1$; the other zeros are points where $\sin \beta_1 s = 0$, and the variation of this term produces a rapid alternation as $\lambda \to 0$. The value of λ for the first zero is independent of the thickness of the dielectric, the others are dependent on it.

Expressions similar to those for H-waves can be obtained for the various field components in each zone. The electric vector in this case is not confined to one plane, the lines of electric force being three dimensional twisted curves whose transverse and longitudinal components obey different boundary laws. This being so the relations of gradient of E at a boundary are not so simple as for the parallel wire system and for H-waves in the wave-guide. The significant parts of the relations are

$$E_{z0} \sim \cos\beta z,$$

$$E_{\rho 0} \sim E_{\varphi 0} \sim \beta \sin\beta z,$$

$$H_{\rho 0} \sim H_{\varphi 0} \sim \sin\beta z,$$

$$E_{z1} \sim \frac{\beta}{\beta_1} R' \cos(\beta_1 s + \varphi'),$$

$$E_{\rho 1} \sim E_{\varphi 1} \sim \frac{\beta}{\beta_1} \beta_1 R' \sin(\beta_1 s + \varphi'),$$

$$H_{\rho 1} \sim H_{\varphi 1} \sim \frac{\beta}{\beta_1} \varepsilon R' \sin(\beta_1 s + \varphi'),$$

where $$R' = \sqrt{\sin^2\beta z_1 + \frac{1}{n^2}\cos^2\beta z_1}$$

and $$\tan\varphi' = n \tan\beta z_1, \qquad \text{etc.}$$

All the transverse components are continuous at the boundary; for the longitudinal component there is continuity of displacement. The ratio of boundary gradients for E_ρ and E_φ

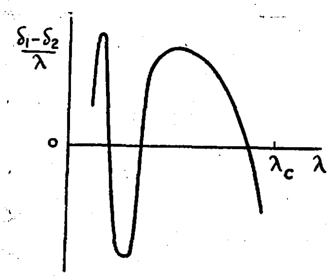

Fig. 20.

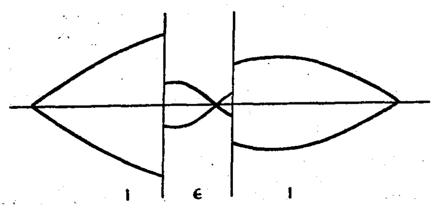

Fig. 21.

is $\beta_1^2/\beta^2\varepsilon$, which is not equal to unity. Thus the simple diagrammatic method of tracing the wave distribution is not now available. However, the gradient of E_z is continuous at the boundary although actual intensities are in the ratio of ε. These facts enable us to draw rough distribution diagrams such as fig. 21, which represents E_z.

The relative simplicity of the components for an H-wave is due to the fact that we have the permeability terms unity. Had this not been so the introduction of a term μ for the dielectric would have made the equations for H-waves similar to those for E-waves with ε replaced by μ.

Chapter 5.

FURTHER MEASUREMENTS ON DIELECTRICS.

17. Displacement Method for Solid Dielectrics - Method B.

The work of the preceeding chapter provides a mental picture of what happens inside the tube when a cylinder of dielectric is inserted and also supplies equations from which values of ε can be calculated.

As a first attempt a short cylinder of paraffin wax was moulded, 4 cm. long and a sliding fit for the tube. By means of the moving probe curves were obtained of the field distribution on both sides of the wax for various positions of the slab. This method, however, was tedious, and it was considered preferable to measure accurately resonance positions of the reflector. It was found that the most satisfactory method of indicating resonance was by observing the reaction on the anode current of the oscillator. The no-load current was balanced out by the simple circuit shown in fig.22, and the increase at resonance observed on a 0-500 $\mu a.$ meter. The reading on the large meter is reduced to zero by the 600 ohm variable resistance, and then the microammeter is switched in. By this means it is possible rapidly to draw a shift curve - i.e. a curve relating resonance position of the reflector to the position of the dielectric slab. This was done first of all for the E_0-wave. The slot along the top of the tube allows the wax to be moved and its position to be read by a scale.

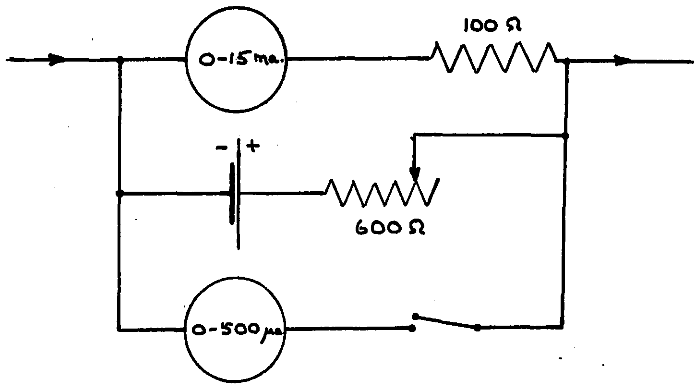

Fig. 22. Arrangement for detecting resonance point.

The wax was moved in steps of 1 cm., the resonance position of the piston determined for each step, and a "shift curve" obtained. When the approximate positions for maximum and minimum piston movement were located, smaller steps were taken and the turning values of piston position determined accurately. Before and after these measurements the resonance position of the piston was found for the empty tube, and the wave-length of the oscillator determined. The work of section 16.2 shows that this curve will approach a straight line as the exciting wavelength approaches a definite value either from above or below. Fig. 23 shows a number of these curves for different wavelengths. It will be seen that the curves are periodic and skew, like the theoretical curve of fig. 13, and degenerate into practically a straight line at a wavelength of 19·35 cm. The value of n given by equation (37) is unity at this point. For wavelengths below it $n>1$, for those above it $n<1$.

If δ is the piston shift due to the insertion of the dielectric, turning values of δ are given by equations (25), (26). If $\delta_{max.}$ or $\delta_{min.}$ is determined experimentally ε can be obtained from the appropriate equation. Either gives an awkward transcendental equation for ε since both n and β_1 are functions of ε, but, by using both, an explicit solution can be obtained as follows:

Dividing the two equations gives

$$\frac{\tan\frac{1}{2}\beta(s_1+\delta_1)}{\tan\frac{1}{2}\beta(s_1+\delta_2)} = n^2 = \left(\frac{\varepsilon\beta}{\beta_1}\right)^2.$$

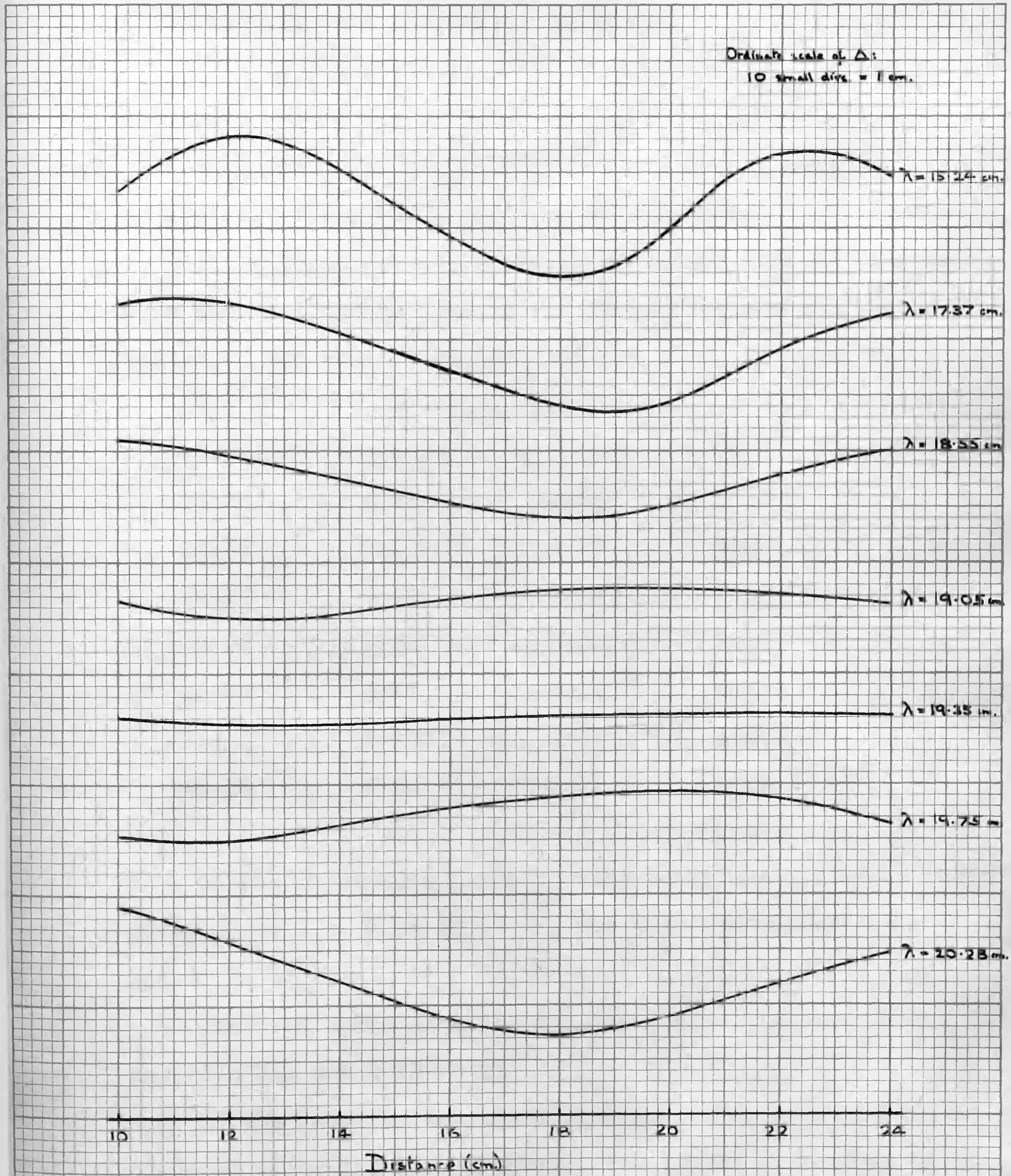

Fig. 23. Shift curves for paraffin wax--E_0 waves.

On multiplying the two equations we get

$$\beta_1 = \frac{2}{s_1} \tan^{-1}\left\{ \tan\tfrac{1}{2}\beta(s_1+\delta_1) . \tan\tfrac{1}{2}\beta(s_1+\delta_2)\right\}^{\frac{1}{2}},$$

and hence

$$\varepsilon = \frac{2}{\beta s_1} \tan^{-1}\left\{ \tan\tfrac{1}{2}\beta(s_1+\delta_1) \tan\tfrac{1}{2}\beta(s_1+\delta_2)\right\}^{\frac{1}{2}} \cdot \left[\frac{\tan\frac{1}{2}\beta(s_1+\delta_1)}{\tan\frac{1}{2}\beta(s_1+\delta_2)}\right]^{\frac{1}{2}}, \quad (41)$$

an explicit value for ε in terms of measurable quantities $\lambda, s_1, \delta_1, \delta_2$.

Using formula (41), a number of determinations of ε were made for readings between 15 and 21 cm. wave-length. The values of the quantities involved are shown in table 4.

Table 4.

λ (cm.)	$\delta_{max.}$ (cm.)	$\delta_{min.}$ (cm.)	ε	$s_1 = 4{\cdot}07$ cm.
16·20	3·77	2·54	2·16	
17·37	4·43	3·33	2·25	
18·55	4·88	4·18	2·27	
18·92	4·54	4·26	2·14	
19·05	4·87	4·66	2·22	
19·40	5·13	5·06	2·24	
20·28	6·86	5·41	2·25	
		Mean	2·22 ± 0·01	

In the first five lines of this table $n>1$ and hence (26) gives $\delta_{max.}$, i.e. δ_1 is $\delta_{max.}$. In the last two cases $n<1$ and δ_1 is $\delta_{min.}$

The mean value obtained for the dielectric constant of paraffin wax was 2·22 ± 0·01.

Of the recently developed plastics, one, polystyrene, is of great value for high-frequency insulation on account of its low power factor *.

* Most of the high-frequency insulation in the apparatus described here is of polystyrene.

It was thought of interest to measure its dielectric constant at these frequencies. From a 3-cm. slab of the material supplied under the trade name of "Trolitul" a cylinder was cut and machined to the 7-in. diameter of the tube and was used in the same way as the paraffin wax cylinder.
Some of the shift curves obtained with this are shown in fig. 24, and values obtained are given in table 5.

Table 5.

λ (cm.)	$\delta_{max.}$ (cm.)	$\delta_{min.}$ (cm.)	ε	$s_1 = 2{\cdot}90$ cm.
17·01	3·63	2·06	2·42	
18·10	3·88	2·81	2·41	
19·01	4·08	3·53	2·44	
19·07	3·98	3·71	2·39	
20·15	5·53	4·55	2·52	
20·26	5·77	4·50	2·53	
20·39	5·80	4·58	2·51	
20·87	6·88	4·84	2·50	
		Mean	2·47 ± 0·01	

For the first four sets of readings in this table $n > 1$, and $n < 1$ for the others.

The mean value obtained for the dielectric constant of polystyrene was 2·47 ± 0·01. To compare this value with that for optical frequencies a prism of polystyrene was made. The square of the index of refraction obtained with a spectrometer for the Na D lines was 2·51.

If this method is to be used with H-waves the explicit equation for ε corresponding to (41) is readily shown to be

$$\varepsilon = \left(\frac{k\lambda}{2\pi}\right)^2 + \left(\frac{\beta\lambda}{2\pi}\right)^2 \frac{\tan\frac{1}{2}\beta(s_1+\delta_1)}{\tan\frac{1}{2}\beta(s_1+\delta_2)} . \qquad (42)$$

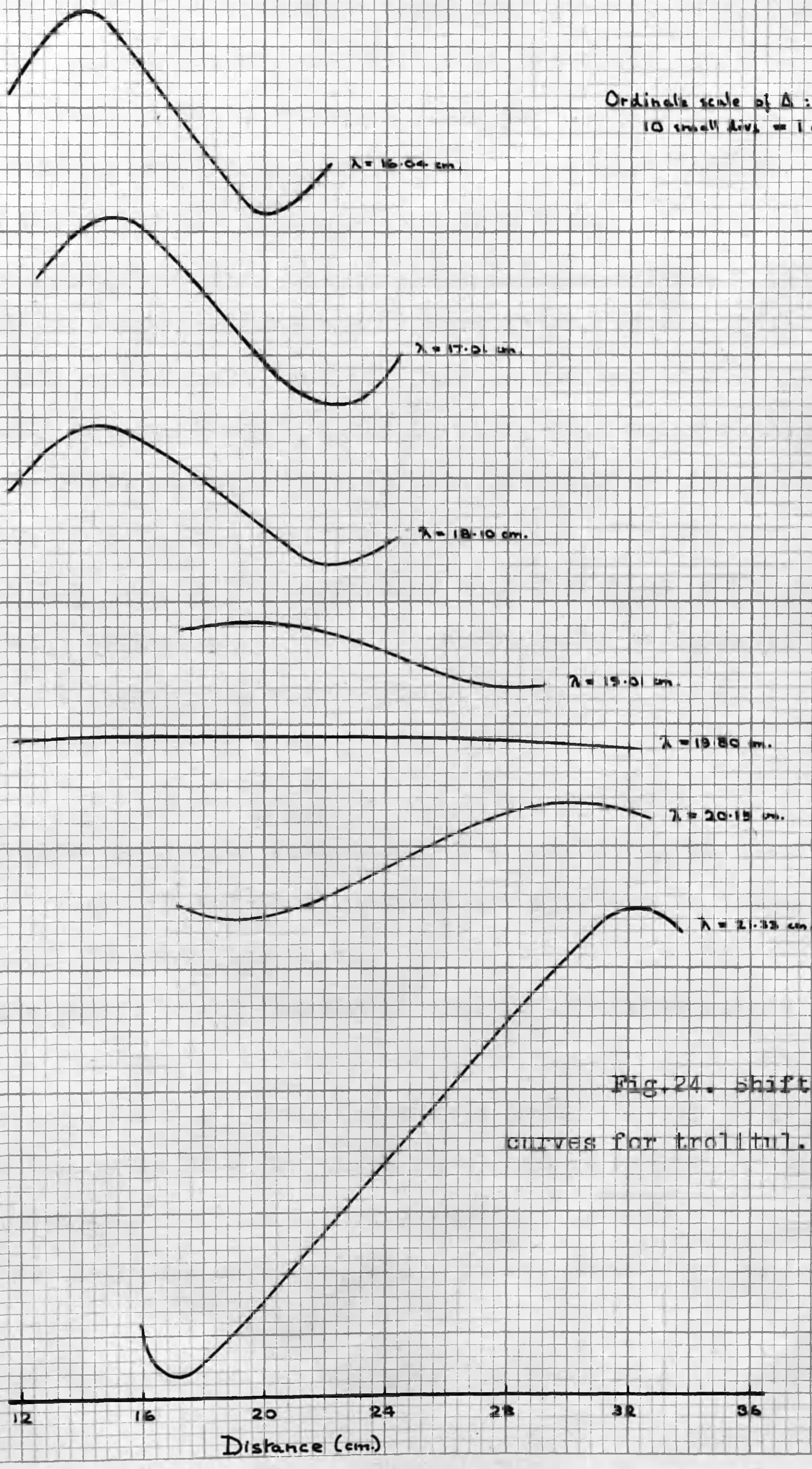

Fig.24. Shift curves for trolitul.

A number of shift curves were taken for H_1-waves, using the paraffin wax and polystyrene cylinders, but these again showed irregularities, presumably due to the same reason as that noted in section 6. It was not considered that reliable results could be calculated from them.

18. Straight-Line-Shift Method for Solid Dielectrics - Method C.

It is some inconvenience to have to remove the dielectric after each measurement, and it would be simpler if the difference only between δ_1 and δ_2 could be used, this being obtained from the shift curve. This is made possible by means of equation (40). That equation is again not suitable for calculation, but in the particular case for which $n = 1$, $\Delta = \delta_1 - \delta_2$ becomes zero, i.e. the shift curve degenerates into a straight line. The wavelength at which this occurs has already been given in equation (39)

$$\lambda = \frac{2\pi}{k}\sqrt{\frac{\varepsilon}{\varepsilon+1}} , \qquad (39)$$

and if this wavelength is determined ε can easily be determined. Figs. 23 and 24 illustrate the approach to the condition of straight line shift.

The points on the curves of fig. 25 are taken mainly from the readings of tables 4 and 5, values of Δ/λ being plotted against λ. From the curves drawn through these points the value of λ for which $\Delta = 0$ can be determined by interpolation. For an actual determination only a few points close to $\Delta = 0$ are required, and a linear interpolation is sufficient.

For the paraffin wax cylinder the value of λ for which $\Delta = 0$

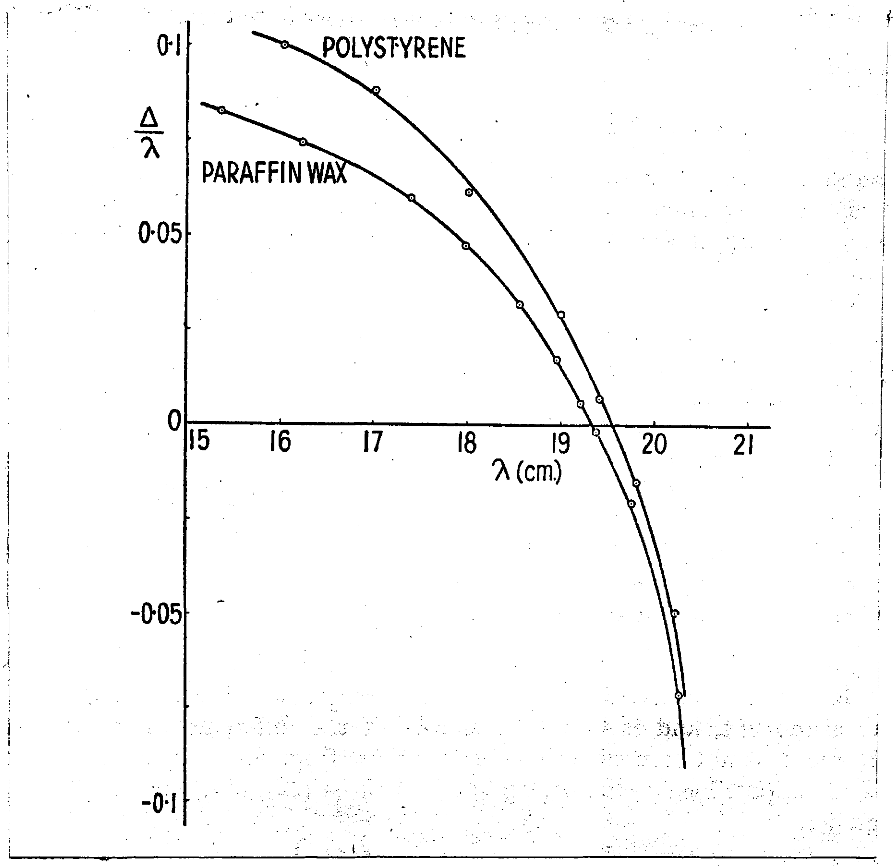
0·1
0·05
0
-0·05
-0·1
Δ/λ
POLYSTYRENE
PARAFFIN WAX
15
16
17
18
19
20
21
λ (cm.)

Fig. 25.

was found to be 19·30 cm., which, using equation (39), gives ε = 2·21. For the polystyrene cylinder this particular wavelength was 19·62 cm., which corresponds to a value of ε = 2·47. These results agree well with those obtained by method B.

It should be noted that by this method ε can be found at only one wave-length, this being determined by ε itself and by the tube radius. If a range of wave-length is required, as in the investigation of an absorption band, method B is suitable.

The H-waves are not suitable for use with method C, since for H-waves n is given by

$$n = \sqrt{\frac{\varepsilon - \left(\frac{k\lambda}{2\pi}\right)^2}{1 - \left(\frac{k\lambda}{2\pi}\right)^2}}, \qquad \ldots\ldots\ldots\ldots\ldots(35)$$

and as, from this expression, n is always $> \sqrt{\varepsilon}$ there is no point at which $\Delta = 0$.

19. Straight-Line-Shift Method for Liquid Dielectrics - Method D.

An attempt was next made to adapt method C to the measurement of dielectric constants of liquid dielectrics. The method was to use a short cylindrical container which could be filled with the liquid and used in the same way as the dielectric slabs previously used.

King has shown in his analysis of the corresponding problem in the Lecher wire system that, if the ends of the dielectric sample have thin retaining walls, each of these can be regarded as a small lumped susceptance, $-ib$, across the wires at that point. This is realizable as a small condenser across the wires, and, although the same is not possible for the wave guide, the concept of a lumped susceptance across a section of the tube is mathematically identical. King's equation corresponding to (22) is

$$(Nb + n\cot\beta_1 s_1)(\cot\beta s' - \cot\beta s_2) + \cot\beta s'\cot\beta s_2 + n^2 - 2Nnb\cot\beta_1 s_1 - N^2b^2 = 0, \tag{43}$$

where N is the characteristic impedance of the line. If again s_2 is replaced by $s' - (s_1+\delta)$ King states that the maximum value of δ is given by the equation

$$\tan\tfrac{1}{2}\beta(s_1+\delta_1) = -Nb + n\tan\tfrac{1}{2}\beta_1 s_1 . \tag{44}$$

In fact this is not necessarily a maximum but is a turning value. The other turning value can be shown to be

$$\tan\tfrac{1}{2}\beta(s_1+\delta_2) = \frac{1}{Nb + n\cot\tfrac{1}{2}\beta_1 s_1} . \tag{45}$$

These equations correspond to (26) and (25) and the question of maximum and minimum has been discussed in section 14.1. Nb can be found by measuring the maximum or minimum shift for the empty cell and putting $\varepsilon = 1$ in (44) or (45). As before, equations (44) and (45) are not amenable to calculation, but if we obtain shift curves for the cell filled with dielectric and from them obtain, as in C, the wave-length for which $\Delta = 0$, then at this point, although n will not be equal to unity because of the effect of the cell walls, it will not be far different from unity. To find this difference put $\delta_1 = \delta_2$ in (44) and (45), and we get

$$(Nb + n\cot\tfrac{1}{2}\beta_1 s_1)(-Nb + n\tan\tfrac{1}{2}\beta_1 s_1) = 1,$$

whence, for Nb small, $n^2 - 2nNb\cot\beta_1 s_1 = 1$, i.e., $$n \doteqdot 1 + Nb \cot \beta_1 s_1 . \quad \text{............}(46)$$

To find Nb put $\varepsilon = 1$ in (44) and (45); then for δ_1' and δ_2' small

$$Nb = -\tfrac{1}{2}\beta\delta_1' \sec^2 \tfrac{1}{2}\beta s_1$$

and $$Nb = -\tfrac{1}{2}\beta\delta_2' \operatorname{cosec}^2 \tfrac{1}{2}\beta s_1 ,$$

whence $$Nb \cos\beta s_1 = -\tfrac{1}{2}\beta(\delta_1' - \delta_2') = -\tfrac{1}{2}\beta\Delta' \quad \text{............}(47)$$

The quantity Δ' is the difference between maximum and minimum shifts produced by the empty cell, and, if it is measured at the appropriate wave-length, Nb can be determined from (47). A sufficiently accurate value of β_1 for use in (46) can be got by finding ε from equation (39), which is now only approximately true, viz.,

$$(\lambda)_{\Delta=0} \doteqdot \frac{2\pi}{k}\sqrt{\frac{\varepsilon}{\varepsilon+1}} . \quad \text{............}(48)$$

n can now be found from (46), and hence ε from equation (37).

The cell used is made from celluloid sheet in the form of a cylinder 4 cm. long and a sliding fit in the tube, and is fitted with a small filling plug. It was filled with the liquid paraffin used previously and from shift curves taken with it the curve of fig.26 was constructed.

From this curve for $\Delta = 0$ the value $\lambda = 19{\cdot}29$ cm. was obtained. At this wave-length a shift curve was drawn for the empty cell which gave for Δ' a value of 0·21 cm. The first approximation to ε from (48) is 2·21. Hence, using equations (46) and (47), we get $n = 0{\cdot}997$. Using this value of n and putting $\varepsilon = 2{\cdot}21 - \eta$ in (37) we get $\eta = 0{\cdot}02$. Hence $\varepsilon = 2{\cdot}19$, which agrees with the value obtained in A.

It is to be noted that if the dielectric constant of the

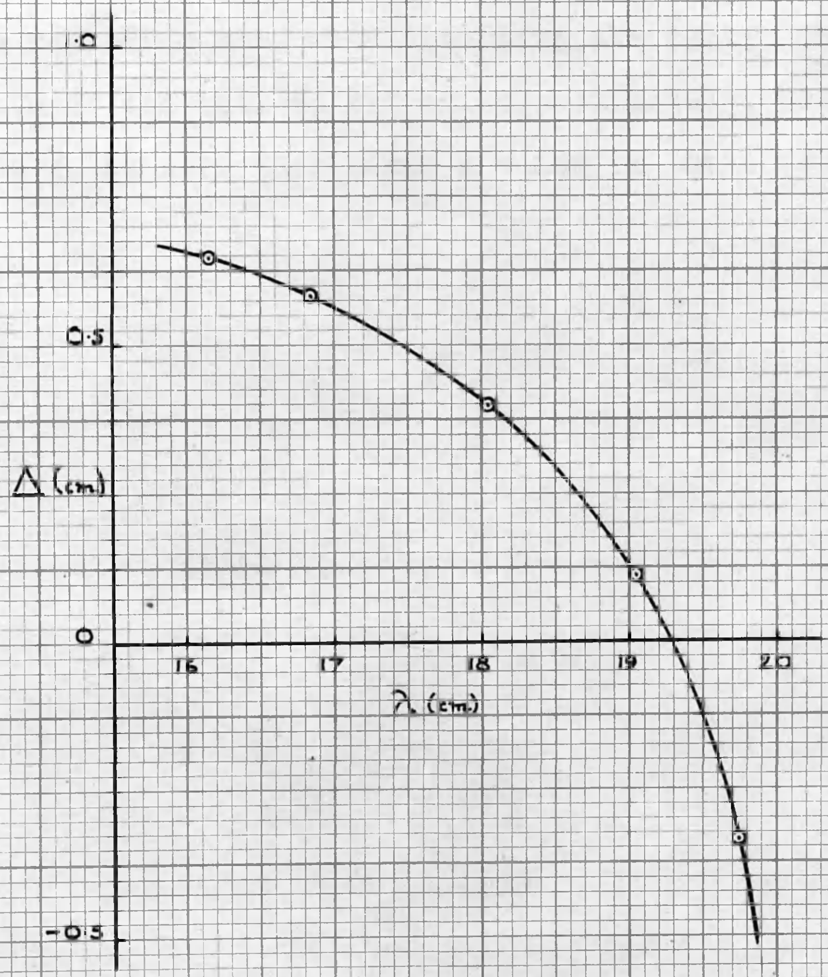

Fig. 26.

liquid is already known approximately (e.g. its low-frequency value or its optical value) the correction to be made can be reduced considerably by choosing the cell length such that $\cot\beta_1 s_1$ in (46) is small. If the value of this term is large the approximations are of little value. A rough calculation was made regarding this when designing the cell; the internal length of the cell is 3·7 cm. approximately, and at the point where Δ is zero this gives a value of $\cot\beta_1 s_1$ equal to 0·13.

Chapter 6.

GENERAL ANALYSIS OF RESULTS.

20. Accuracy of the Dielectric Measurements.

Four methods have been described of measuring dielectric constants for microwaves; of these the first and last are suitable for liquids and the other two for solids. The experimental results obtained by these methods are collected in table 6.

Table 6.

Substance.	Dielectric constant by method:			
	A	B	C	D
Liquid paraffin.	2·191 ± 0·003			2·19
Paraffin wax.		2·22±0·01	2·21	
Polystyrene.		2·47±0·01	2·47	

The accuracy of these results will now be discussed.

A. Individual readings obtained in A showed a maximum variation from the mean of 1·4 per cent. It is considered that a considerable part of this variation is due not to errors in measurement, but to distortion of the wave by slight deformations in the tube. The tube used in the experiments had evidently suffered previous vicissitudes, but it is unlikely that the mean values are appreciably affected.

B. Again the dispersion of the results is largely due to tube irregularities, but the probable error shown is again reasonably small.

C. On account of the form of (39) the error in method C caused by an error in $(\lambda)_{\Delta=0}$ is rather large. For $\varepsilon = 2$ a change of 1 per cent in $(\lambda)_{\Delta=0}$ produces a 6 per cent. change in ε. From a large-scale curve it was found possible to interpolate for $(\lambda)_{\Delta=0}$ to 0·1 per cent., and if, on the basis of the preliminary measurements, we assume that wavemeter readings are correct to 0·25 per cent., the possible error in ε is of the order of 2 per cent. The consistency of results suggests that the actual error is much less than this.

D. The same remarks apply as to method C. Also if the length of the cell is suitably chosen the errors introduced by the approximations made are small, and comparison of the results obtained with that of A shows a satisfactory agreement.

The method is of little value for liquids of high dielectric constant such as water and polar mixtures. The variation of ε with $\frac{\varepsilon}{\varepsilon+1}$ then becomes large, and large errors in ε are caused by small errors in $(\lambda)_{\Delta=0}$.

21. Consideration of Results.

The results for liquid paraffin and paraffin wax are within the usual range for hydrocarbons of 2·1 to 2·3. The composition of paraffin wax being indefinite, the result obtained is of value merely in indicating the order of the dielectric constant at these frequencies. The values of $2{\cdot}191 \pm 0{\cdot}003$ and 2·19 for liquid paraffin compare with Müller's[19] value $2{\cdot}18 \pm 0{\cdot}04$ obtained by Drude's second method at 60 cm. wavelength. The optical refractive index for the for the Na D lines was measured using a spectrometer and a hollow prism filled with the liquid. The dielectric constant is the square of the refractive index and was here found to be 2·20, exactly Müller's value for the Na lines. The measurement at a wavelength of 45·7 m. gave 2·18. Liquid paraffin being non-polar, no dispersion should occur, but the difference between the values for the two frequencies is slight and, being within the estimated error, cannot be said to be significant.

Published values for the dielectric constant of polystyrene do not show entire agreement, the variations being due, perhaps, to difference in purity or in the state of polymerization, for the substance is not a pure chemical compound, being a mixture of chain molecules of different lengths. The value given in a descriptive pamphlet on "Distrene," the British product, is 2·3 (at $800-75.10^4$ c./sec.), that by Race and Leonard[20] 2·4 (at 10^6 c./sec.) for the German Polystyrol, and by Matheson and Goggin[21] 2·55-2·60 (at $60-2.10^7$ c./sec.). A value of 2·5 would seem to be a good average. The result of 2·47 obtained here indicates that no large dispersion occurs at frequencies corresponding to microwaves. To compare this value with that for optical frequencies a prism of polystyrene ("Trolitul") was made. The square of the index of refraction for the Na lines obtained with a spectrometer was 2·51, the same value as obtained by Matheson and Goggin. The difference between the two values is again too small to be significant.

22. Experiments on Wave Distribution inside the tube.

The consistency of the foregoing measurements is a sufficient proof of the correctness of the theory of sections 14 and 16, on which the measurements by methods B-D are based. There remain interesting points in the theory which will be demonstrated.

The curves of figs. 23 and 24 show the variation in the form of the shift curves with wavelength, and the increasing skewness of these curves as the wavelength alters from the straight line value. The values of n for the readings of table 4 have been calculated and are shown graphically in fig. 27.

It was shown in section 14.2 that for maximum and minimum reflector displacement the wave distribution is symmetrical with respect to the dielectric slab (see fig. 17).
By means of the probe moving along the tube through the slot the radial electric field on both sides of the dielectric slab can be measured. Figs. 28 and 29 illustrate the results of such measurements, fig.28 showing the slab in the position for minimum piston displacement, and fig. 29 the slab in the position for maximum piston displacement. The abscissae are distances along the tube from an arbitrary origin, the ordinates are microammeter readings proportional to the square of the field. The symmetrical nature of the distribution is well evidenced. As in the theory, for minimum displacement the first node is at a distance between $\frac{1}{4}\lambda_t$ and $\frac{1}{2}\lambda_t$ from the face of the slab, and for maximum displacement between 0 and $\frac{1}{4}\lambda_t$.

To demonstrate the particular case for which the thickness of the dielectric slab is a multiple of $\frac{1}{2}\lambda_{t_1}$(section 14.5 & fig.18)

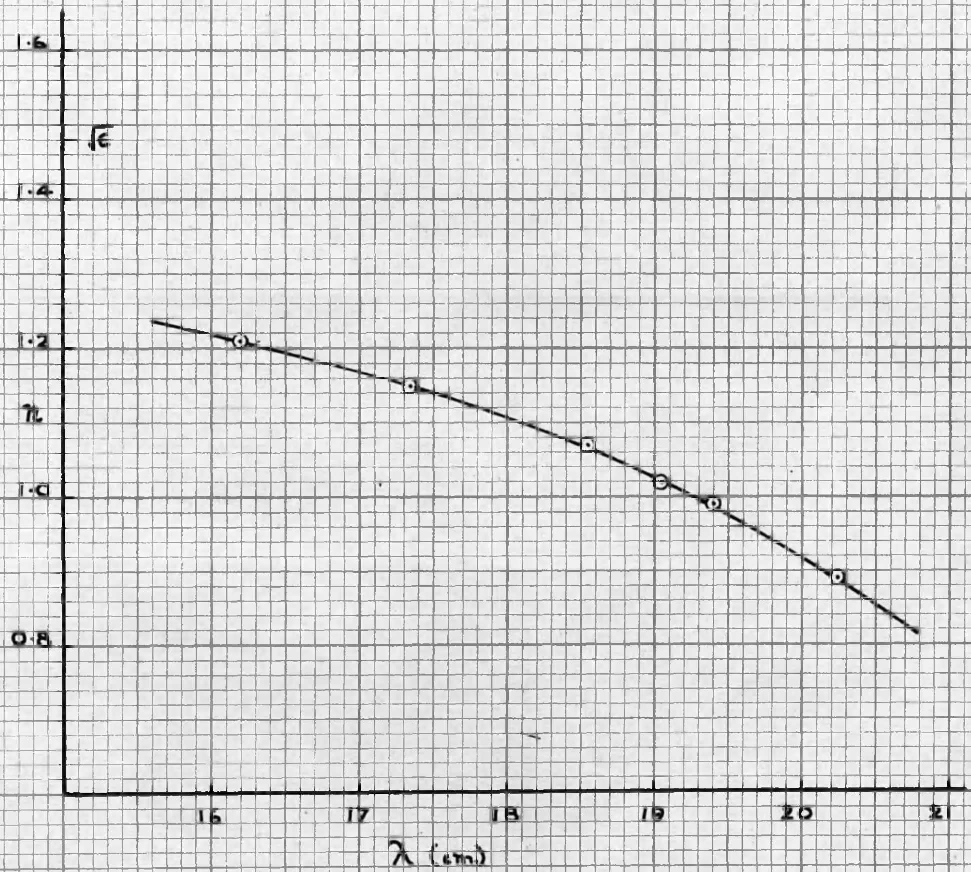

Fig. 27.

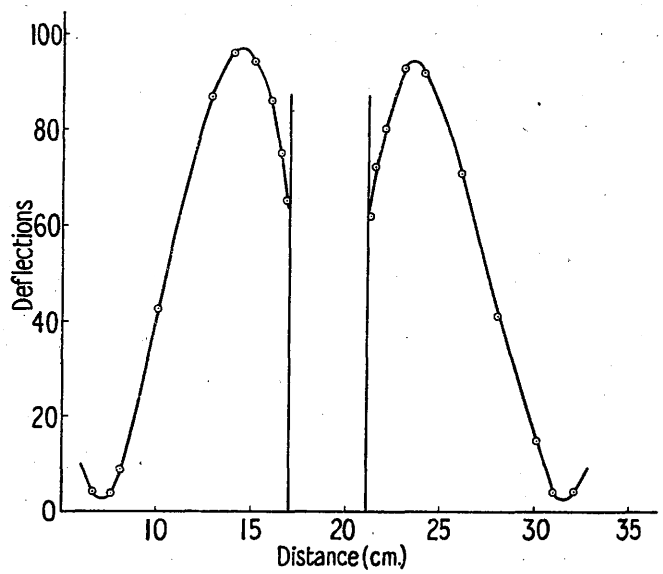

Fig. 28.

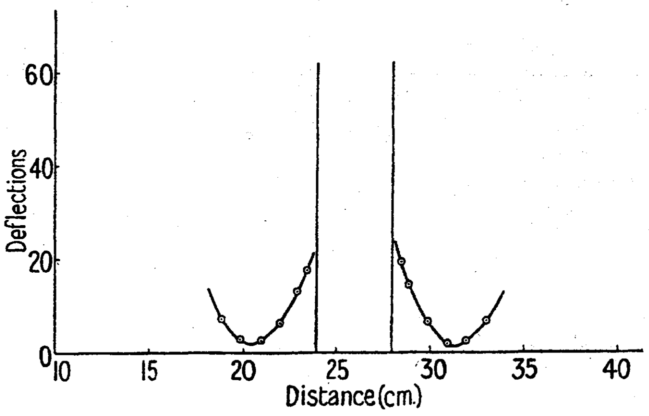

Fig. 29.

Experimental verification of wave distributions of Fig. 17.

another cylinder of paraffin wax was made, of length 6·75 cm. Taking for the dielectric constant the value 2·22 found in B, an oscillation of free space wave-length 17·39 cm. will give an E_0-wave in the tube such that $\frac{1}{2}\lambda_{t_1}$ is equal to the length of the cylinder. The oscillator was set as nearly as possible to this wave-length, and it was verified that the shift curve then obtained was substantially straight. By means of the moving probe the field on both sides of the wax was plotted, and this is shown in fig. 30. The figure demonstrates that the parts of the wave on the two sides of the dielectric are complementary, the external effect of the dielectric being to divide the original wave into two parts and separate them. The amplitudes are not exactly equal, as they should be, but are roughly so.

23. General Conclusions.

When the work described here was commenced there were few published papers on wave guides, and few details. In the interval activity in this field has greatly increased, and it is interesting to note that others, for example Clavier and Altovsky[22], have used experimental arrangements and encountered difficulties very similar to those described in sections 3, 4 and 6. So far no others (excepting reference 10) have used the wave guide in measurements of dielectric constant, although attention has been drawn to its possibilities in an article by Hartshorn in the latest (1939) volume of Reports on the Progress of Physics.

It is considered that the results obtained have fully

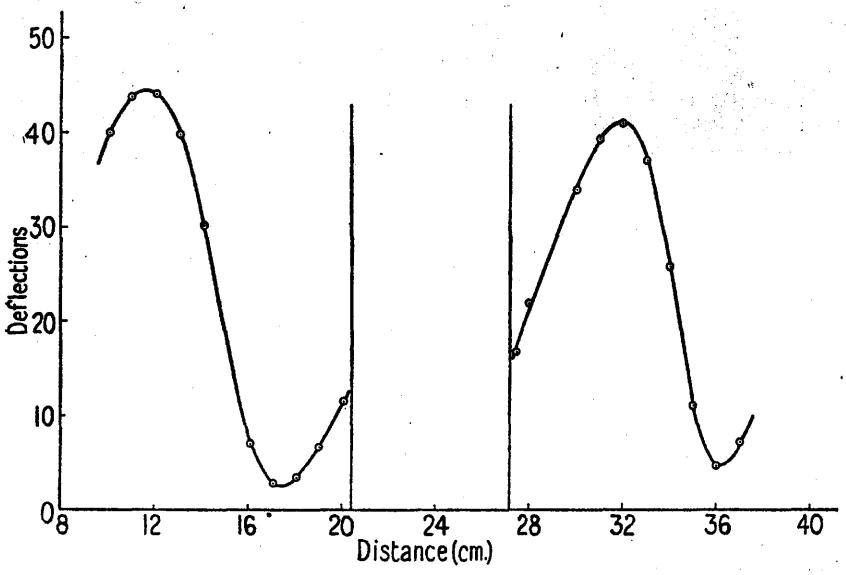

Fig. 30. Experimental verification of wave distribution of Fig. 18(a).

justified the expectation with which the work was begun. Since then, however, advances have been made in the technique of the generation of microwaves, and now appreciable power can be generated without difficulty at wavelengths of a few centimetres. It is in measurements at these frequencies - i.e. with centimetre waves - that the wave guide would provide its greatest advantages over the older techniques, since its one drawback at the decimetre wavelengths - its bulk, would then have disappeared. There seems no reason why the methods should not be so extended, and the results obtained here encourage one to expect, with due precautions taken, reliable and accurate results.

It was hoped to proceed to the study of dielectric losses using the wave guide, but this has not yet been done. The parallel wire method of finding losses by measurement of the width of a resonance curve should be capable of modification for this purpose, and experiments along these lines would yield results very valuable in a region of the electromagnetic spectrum which is rapidly increasing in importance.

REFERENCES

(1) W. L. Barrow, Proc. Inst. Radio Engrs 24 1298 (1936).

(2) G. C. Southworth, Bell Syst. Tech. J. 15 284 (1936).

(3) J. R. Carson, S. P. Mead and S. A. Schelkunoff, Bell Syst. Tech. J. 15 310 (1936).

(4) L. S. Nergaard, Proc. Inst. Radio Engrs 24 1207 (1936).

(5) G. C. Southworth, Proc. Inst. Radio Engrs 25 807 (1937).

(6) A. Hund, Sci. Pap. U.S. Bur. Stand. 19 no. 491 (1924).

(7) P. Drude, Z. Phys. Chem. 23 267 (1897).

(8) F. H. Drake, G. W. Pierce and M. T. Dow, Phys. Rev. 34 613 (1930).

(9) W. I. Kalinin, Phys. Z. Sowjet. 10 257 (1936).

(10) E. Kašpar, Ann. Phys., Lpz. 32 353 (1938).

(11) S. K. Mitra and S. S. Banerjee, Nature 136 512 (1935).

(12) E. V. Appleton, J. Inst. Elect. Engrs 71 642 (1932).

(13) R. King, Rev. Sci. Instrum. 8 201 (1937).

(14) R. L. Smith-Rose and J. S. McPetrie, Proc. Phys. Soc. 46 694 (1934).

(15) S. S. Banerjee and R. D. Joshi, Phil. Mag. 25 1025 (1938).

(16) M. Seeberger, Ann. Phys., Lpz. 16 77 (1933).

(17) W. G. Hormell, Phil. Mag. 3 52 (1902).

(18) S. A. Schelkunoff, Proc. Inst. Radio Engrs 25 1457 (1937).

(19) W. Müller, Ann. Phys., Lpz. 24 99 (1935).

(20) H. H. Race and S. C. Leonard, Elect. Engng., N.Y. 55 1347 (1936).

(21) L. A. Matheson and W. C. Goggin, Industr. Engng. Chem. 31 334 (1939).

(22) A. G. Clavier and V. Altovsky, Rév. Gén. de l'Élect. 45 697, 731 (1939).

Copy 1